ELECTROCATALYTIC OXIDATION OF NITRITES ON GLASSY CARBON ELECTRODE MODIFIED WITH COBALT (II) TETRA-CARBOXY PHTHALOCYANINE/ NITROGEN DOPED GRAPHENE OXIDE NANOSHEETS COMPOSITE.

By

TERENCE T NDHLOVU

(R0724518L)

Submitted in partial fulfillment of the requirements for the degree of

Bachelor of Science Honours in Chemical Technology

Department of Chemical Technology

in the

Faculty of Science and Technology

at the

Midlands State University

Supervisor: Mr M. Shumba

Co –Supervisor: Dr T. Mugadza

June 2016

DEDICATION

This dissertation is dedicated to my family who inspired me to acquire education.

ACKNOWLEDGEMENTS

Firstly I wish to thank God for giving me strength, guidance and patience through this journey, my supervisors: Mr M. Shumba and Dr T. Mugadza for their mentoring, patience and support through the entire research. I would also like to thank my colleagues and MSU lab staff for their support. Lastly, I greatly appreciate the love, inspiration, support and encouragement from my family, Thandeka Pilime and friends. May God bless you all abundantly.

ABSTRACT

This research is based on the modification of a glassy carbon electrode with cobalt (II) tetra carboxy phthalocyanine and nitrogen doped graphene oxide nanosheets composite (CoTCPc/N-GONS) was used for the electrocatalytic oxidation of nitrites. The synthesised cobalt (II) tetra carboxy phthalocyanine (CoTCPc) and nitrogen doped graphene oxide nanosheets (N-GONS) were characterized by FTIR spectroscopy, UV-Vis spectroscopy, electrochemical impedance and cyclic voltammetry. The electrode surface area for CoTCPc/N-GONS-GCE was 0.174 cm^2, which was at least twice that of a BGCE indicating that the modified electrode provided larger surface area for electro catalysis. The modified electrode had a surface coverage of $1.22 \times 10^{-13} mol cm^{-2}$. The CoTCPc/N-GONS-GCE had k_{app} and R_{CT} values of $3.64 \times 10^{-6}\ cms^{-1}$ and 145.47 Ω respectively. The electrochemical detection of the nitrite with CoTCPc/N-GONS-GCE was successful producing high peak currents compared to other electrodes. The electrocatalytic oxidation of nitrite was determined to be a 1st order reaction and with a Tafel slope of 270 mV/decade. Limit of detection (LOD) was 2.49×10^{-7} M and Limit of quantification (LOQ) was 8.29×10^{-7} M. The electrode showed good reproducibility with lower oxidation potential at 0.86 V and high sensitivity towards nitrite.

DECLARATION

I, **Terence Tongai Ndhlovu**, hereby declare that I am the sole author of this dissertation. I authorize Midlands State University to lend this dissertation to other institutions or individuals for the purpose of scholarly research.

Signature………………………..

Date……………………………...

This dissertation entitled, **electrocatalytic oxidation of nitrites on glassy carbon electrode modified with cobalt (II) tetra-carboxy phthalocyanine/ nitrogen doped graphene oxide nanosheets composite** by Terence Tongai Ndhlovu meets the regulations governing the award of the degree of Chemical Technology of Midlands State University, and is approved for its contribution to knowledge and literal presentation.

Supervisor…………………………..

Date……………………

Table of Contents

LIST OF ABBREVIATIONS

CoTCPc - Cobalt (II) tetra carboxy phthalocyanine

CoPc - Cobalt phthalocyanine

CV - Cyclic voltammetry

DPV - Differential pulse voltammetry

EIS - Electrochemical impedance spectroscopy

FTIR - Fourier transfer infrared

GCE - Glassy carbon electrode

HOMO - Highest occupied molecular orbital

LOD - Limit of detection

LOQ - Limit of quantification

LUMO - Lowest unoccupied molecular orbital

N-GONS - nitrogen doped graphene oxide nanosheets

UV-Vis - Ultraviolent visible

LIST OF SCHEMES

LIST OF TABLES

LIST OF FIGURES

CHAPTER 1

INTRODUCTION

1.0 Introduction

This chapter highlights the summary of the research, background, phthalocyanines, nitrogen doped graphene nanosheets (N-GONS) and electrochemical techniques.

1.1 Background

There are several analytical techniques used for quantitative determination of nitrite including spectrophotometry, ion chromatography and electrochemical methods [1]. However, these analytical methods usually have expensive equipment, tedious detection procedure and often time consuming. The electrochemical method has been proven to be inexpensive and effective way for quantitative determination nitrites, because of its intrinsic sensitivity and simplicity [2].

1.1.2 Phthalocynanines (Pcs)

Phthalocyanine derivatives, which have a similar structure to porphyrin, have been utilized in important functional materials in many fields. Their useful properties are attributed to their efficient electron transfer abilities [3]. The central cavity of phthalocyanines is known to be capable of accommodating 63 different elemental ions, including hydrogen (metal-free phthalocyanine, H_2-Pc) [4]. A phthalocyanine containing one or two metal ions is called a metal phthalocyanine (M-Pc) [5]. As a result of their high electron transfer abilities, M-PCs have been utilized in many fields such as molecular electronics, optoelectronics, photonics, and electro catalytic properties. The functions of M-PCs are almost universally based on electron transfer reactions because of the 18 π electron conjugated ring system found in their molecular structure.
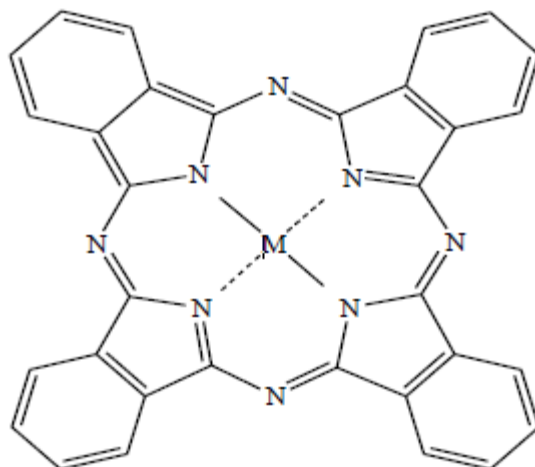
Figure 1.1: General chemical structure of a metallophthalocyanine (MPc)

Properties of MPc molecules are closely related to the metal atom located at the central cavity [6]. Such metal atoms are cobalt, copper, iron and zinc.

1.1.3 Nitrites

Nitrites are crucial ions used in some food additives or to prevent corrosion [1]. The importance of determination of nitrite in water, food and agriculture products which to prevent corrosion, has been widely recognized due to the evidence that nitrites can interact with amine and form carcinogenic compounds of nitrosamines [7]. Nitrites can be introduced into the environment due to different chemical handling activities such as farming.

1.1.4 Nitrogen doped graphene oxide nanosheets (N-GONS)

1.1.4.1 Introduction

Graphene, is a single atom-thick sheet of hexagonally arranged sp^2 – bonded carbon atoms, shows extraordinary electronic, mechanical, optical and potential applications because of its unique properties such as high surface area, high conductivity, mechanical strength [8]. Graphene has potential applications in many fields, such as solar cells, sensors, fuel cells and

drug delivery and biosensor [9]. Doping of graphene with elements like boron, nitrogen, oxygen and sulphur can enhance the electronic properties and chemical reactivity. In particular, nitrogen doped graphene (NG) and boron doped graphene (BG) have been highly used in lithium-ion-batteries, super capacitors, and catalysis for oxygen reduction reaction (ORR) [9–12]. Among these the most important applications of NG is electro catalyst of ORR, because it has ability to replace expensive Pt-based catalyst for fuel cells and metal-air batteries. It has high catalytic activity and superior reliability.

1.1.4.2 Structure

The schematic diagram of the bonding configuration of N atoms in graphene is shown in Fig 1.2 which determines the performance of NG. The configurations of typical N functionalities present in NG includes N atoms doped into graphene basal plane (quaternary N), N atoms in six member ring (pyridinic N) and five member ring (pyrrolic N), among them Quaternary N is believed to be vital for catalytic activity [13].
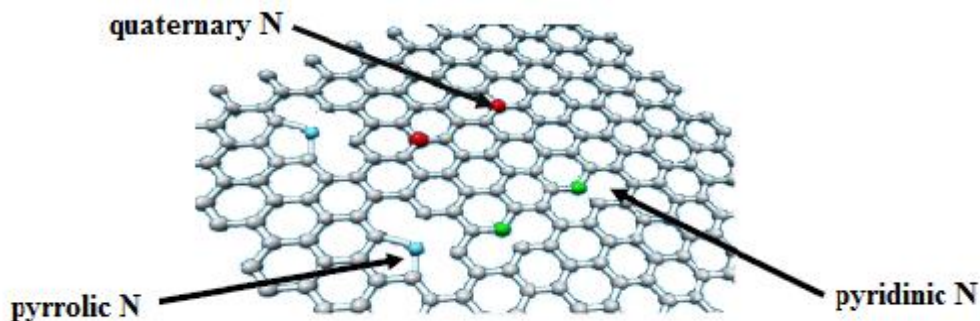
Figure 1.2: Schematic diagram of the bonding configuration of N atoms in graphene [13]

1.1.4.3 General synthesis of nitrogen doped graphene oxide nanosheets.

Generally, there are several major methods like mechanical exfoliation, epitaxial growth bottom up synthesis and chemical reduction of graphene oxide (GO) suspension, which are used to prepare the reduced graphene sheets [12,14,15]. Among them, the chemical reduction of GO results in a bulk quantity and at relatively low cost. GO is mainly synthesized by the Brodie, Staudenmaier or Hummers method. All of them produce GO by the strong oxidation of graphite with acid. GO is highly hydrophilic, and it can be easily exfoliated in aqueous media which are then subjected to chemical reduction to obtain graphene as individual sheets [11,16]. The reducing agents which are mainly used are hydrazine, sodium borohydride, hydroquinone, or strongly alkaline solutions. The chemical reduction of GO results in restoration of sp^2 carbon sites but not all the oxygen functionalities are removed completely and it also leaves a number of defects like vacancies, edge/cracks and adsorbed impurities [15,17]. Many methods have been successfully demonstrated to dope nitrogen atoms into graphene sheets such as thermal annealing of GO in ammonia, chemical vapor deposition by adding ammonia gas (or other nitrogen precursor) and electrical joule heating in ammonia [18,19]. Scheme 1.1 demonstrates the synthesis of nitrogen doped graphene oxide nanosheets.
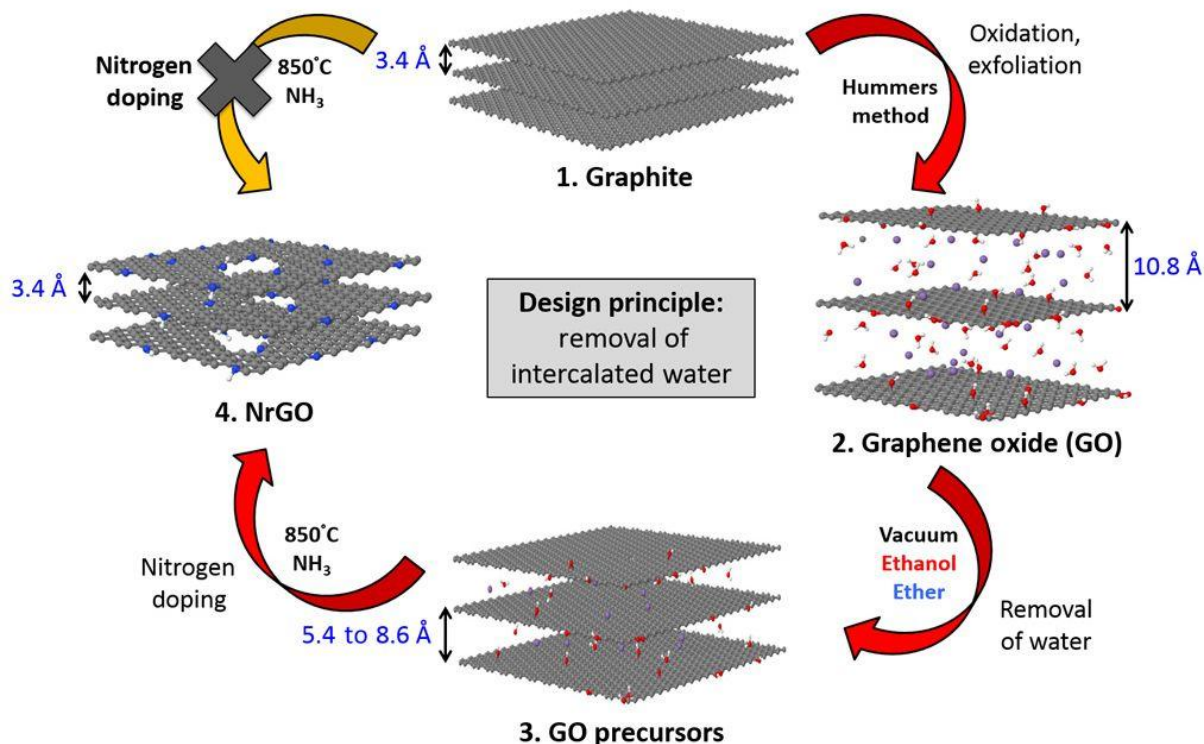
Scheme 1.1: Synthesis of nitrogen doped graphene oxide nanosheets [18].

1.1.5 Voltammetry

Numerous methods for the analysis of nitrites have been developed and reported elsewhere, such as fluorescence spectrophotometry, microchip electrophoresis, thin layer chromatography, UV-Vis, gas chromatography [20]. Compared with other detection techniques, the electrochemical methods are proved to be popular tools ascribed to their advantages of stability, selectivity, and simple and easy fabrication process [21]. Various electrochemically modified electrodes have been explored to detect the content of nitrites in samples. Compared to these methods, the electrochemical method can provide compact, relatively inexpensive, reliable, sensitive and real-time analysis [22]. Moreover, the development of a rapid electrochemical method for nitrite detection without the sample pretreatment prior to analysis and also no interference from other sources (such as nitrate, sulfate and bromate ions) is highly important. Recently, different kinds

of electrochemical nitrite sensors have been fabricated based on the chemical modification of electrode [23].

1.1.6 Electrode modification

When an electrode such as a bare glassy carbon electrode is cover with a layer of water molecules or solvent containing certain species or impurities, the species present in solution will attach to the electrode surface [2]. The presences of such adsorbed species will often modify the electrochemical behavior of the electrode. For example, they may cause the current observed for a given electrochemical process to be much smaller, because they block access to electrode surface [24]. In this research the modification of the electrode with Cobalt (II) tetra-carboxyl phthalocyanine incorporated with nitrogen doped graphene oxide nanosheets is aimed at improving the electrochemical detection of nitrites by the electrode. The modified electrode should exhibit lower peak potential in the detection of nitrites compared to a bare glassy carbon electrode [25]. Modifying an electrode with chemical species that have good electrochemical properties such as conductivity, thermal stability and large surface area will improve the sensitivity and selectivity of the electrode [26].

1.2 Aim of the study

• To determine the electrocatalytic oxidation of nitrites on glassy carbon electrode modified with cobalt (II) tetra-carboxy phthalocyanine/ nitrogen doped graphene oxide nanosheets composite.

1.3 Objectives

- To synthesise cobalt (II) tetra-carboxy phthalocyanine (CoTCPc).

- To characterize the electrode modifiers with FTIR, UV-Vis, cyclic voltammetry, differential pulse voltammetry and electrochemical impedance spectroscopy.

- To modify glass carbon electrode with cobalt (II) tetra-carboxy phthalocyanine incorporated with nitrogen doped graphene oxide nanosheets (CoTCPc/N-GONS).

- To evaluate the effect of pH, scan rate and concentration on peak currents and peak potentials.

- To determine the apparent rate constant (k_{app}), Tafel slopes, and relative catalytic effects of the (CoTCPc/N-GONS-GCE).

1.4 Problem statement

Industrial processes have been known to generate large effluents that contain high levels of toxic heavy metals and organic pollutants [27]. The presence of these organic and inorganic (for example cadmium, chromium, mercury, perchlorates and of interest in this research nitrites) contaminants in water sources has huge environmental, public health and economic impact. Monitoring and removal from drinking water of these contaminants is associated with high costs. They also result in an imbalance of the aquatic life; affect ground water, commercial fishing, recreational and cultural activities associated with lakes and river water. Therefore there is need for monitoring and remediation of nitrites in the water resources using low cost, fast and easy methods which can find applicability in both rural and urban areas. The most employed

techniques are chromatography and spectrometry, which require intensive sample preparation, require experienced personal and are expensive [2,7,28]. In the recent years electrochemical techniques have proved to be fast, reliable and cost effective as compared to the traditional conventional techniques [29–31]. There is still need to improve the electrode modifying material for the oxidative detection of nitrites. This research is aimed at contributing to the improvement of electrode modifiers that is cheap and has excellent electrocatalytic properties.

1.5 Justification

Traditional analytical techniques for the determination of nitrites are usually time consuming as they are based on discrete sampling methods followed by laboratory analyses [22]. Electrochemical techniques represent an important subclass of methods that do not require extensive sample pre-treatment and the electrode is used as the transduction element. They meet the cost, size and power requirements to even perform on-site analysis. There is still need for development electrochemical determination of nitrites in the area of electrochemistry. These include selectivity, stability and to meet challenges posed by the environmental samples [28,32–34]. Characteristics that make electrochemical methods more favourable include low cost instrumentation, sensitivity and selectivity, minimal space and power requirements. Also by providing fast processing of the analytical information in a   safe and cost effective manner, electrochemical techniques provide direct and reliable nitrite detection. Incorporation of the glassy carbon electrode with nanomaterials makes this technique to be a cheap, reliable and fast method of detection of nitrites [30].

1.6.0 Literature review

1.6.1 Summary

Metallophthalocyanines (MPcs) carrying electro-active metal centres have attracted the attention of many researchers due to their excellent electro-catalytic properties. Their chemical and physical properties can also be altered by varying the substituent on the phenyl rings [35]. These include groups such as amino, sulfo, hydroxyl and for this study carboxyl. The carboxyl groups provide sites for the phthalocyanine to chemically link with other compounds [36]. In this study CoTCPc is chemically linked to another electro-active specie nitrogen doped graphene oxide nanosheets. This improves chemical and physical properties, resulting in improving catalytic activity and reduced over potential for oxidative determination of nitrites.

1.6.2 Phthalocyanine (Pc).

1.6.2.1 Discovery

The macromolecules were accidentally discovered in year 1928 at the works of Scottish Dyes Ltd. The discovery came as a result of passing ammonia gas on molten phthalic anhydride in an iron vessel for the synthesis of phthalimide; there appeared a blue coloured impurity in the reaction mass [37]. Dunworth and Dreseher properly repeated the reaction of phthalimide with iron compounds to establish the synthesis of this blue green compound. In 1929 the first patent was issued with respect to compounds that we now know as phthalocyanines, to Dandrige, Drescher and Thomsan of Scottish Dyes Ltd. The patent based on the claim of the reaction of ammonia or primary monoamines of aliphatic series or of benzene or naphthalene series on phthalic anhydride, phthalimide or mono or diamide of phthalic acid in presence of iron, nickel or cobalt in the form of metal or compounds [38,39]. From 1929 till 1933 non of the scientist working with the compound attempted to determine the structure of this compound when

professor Linstead at the University of London determined and proudly announced the structure of Pc and metal Pcs in the year 1933 and 1934. Thus 1934 was the year when the discovery of Pc class of organic compounds terminated [40–42].

1.6.2.2 Structure

Phthalocyanine has a molecular formula $C_{32}H_{18}N_8$ or $(C_8H_4N_2)_4H_2$ and has a grouping of 4 isoindoline units arranged in the form of a planner ring structure [29]. Metal phthalocyanine (MPc) is derived by replacement of the two hydrogen atoms in the centre by metal atom [3,10].

phthalocyanine   Metallo phthalocyanine
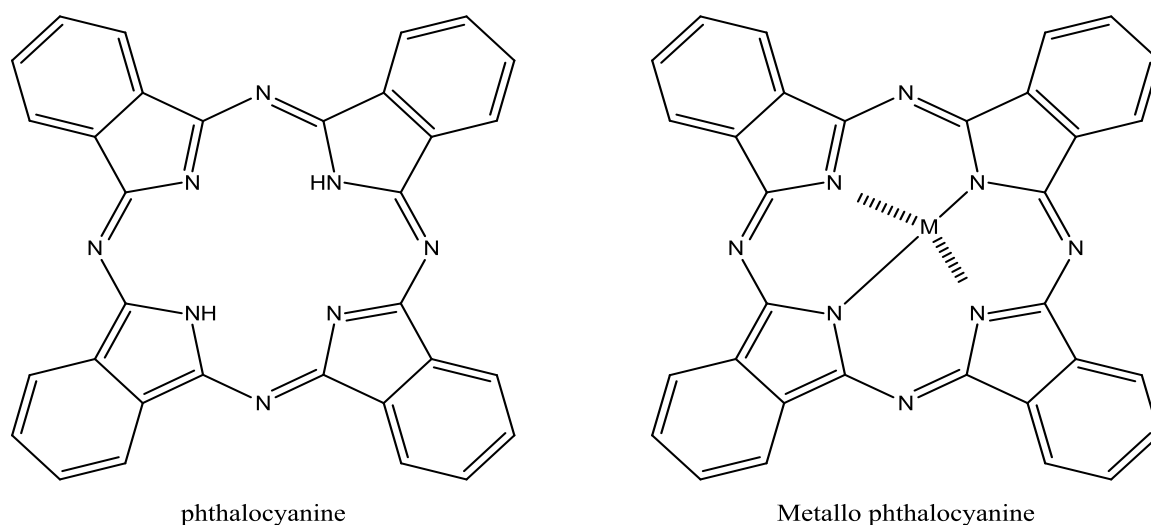
Figure 1.3: General structure of phthalocyanine and metallophthalocyanine.

The colour of the resultant Pc changes with presence of a particular metal at the centre. Generally Pcs and MPcs are stable colour pigments which are very stable against heat (sublimes at 550°C), oxidation, reduction, acids, alkalis and other wear and tear activities [29,36]. The macromolecule has the same resembles to other naturally occurring coloured compounds, like green chlorophyll in each of the plants and red hemin of haemoglobin of red blood cells. All this coloured compounds have the same inner chemical structure, in each of them 4 pyrole units join

to the central metal atom through their nitrogen atom [43]. Phthalocyanines differ only by the presence of 4 benzene rings on the periphery of the pyrolian ring structure and in general this makes phthalocyanines much more stable as compared to the porphirines [38].

1.6.2.3 General application of phthalocyanines (Pcs).

The characteristic properties such as very high thermal stability, intrinsic conductivity, intense colour, electron transfer reactions due the 18π electron ring system which enables various redox activity and other properties, make phthalocyanines suitable form many applications. In particular Pcs attract attention in the field of molecular electronics such as for photovoltaic cells [14,41,44,45], optical displays and organic light emitting diodes. Others include chemical sensors, based on their attractive blue to green colours and excellent fastness to light this makes Pcs suitable for commercial production of dyes, catalysis and synthetic metals [46].

1.6.2.4 General synthesis of Phthalocyanines (Pcs)

Phthalocyanines can be synthesised as metal free or metal substituted compounds [37]. Ever since their discovery, researchers reported quite a number of synthetic methods that involve derivatives that can be applied as precursors [3,47]. These include phthalic acid, phthalic anhydride, phthalonitrile, o-cyanobenzene and o-dibromobenzene. Researchers usually favour the use of phthalonitrile derivatives over those of the inexpensive phthalic anhydride derivatives which are also favourites but produce low yields. However phthalonitrile precursors give a clean reasonable yield and are easy to produce [48]. The product is therefore suitable to carry out further studies, with the exception of the metals mercury ad silver, while compared to some precursor derivatives which a produce a fair yield, but with trace impurities leading to undependable further studies. In this study research a phthalic anhydride, trimellitic anhydride precursor was used.

1.6.2.5 Metal free Substituted phthalocyanines.

Even with earlier difficulties in preparing phthalonitriles, Linstead and Lowe showed that phthalonitrile, upon treatment with sodium or lithium *n*-pentoxide in *n*-pentanol at 135-140 °C produced disodium phthalocyanine, which could be directly demetallated to phthalocyanine with concentrated sulphuric acid. Substituted phthalocyanines are now easy to synthesis by this method since substituted phthalonitriles are ready obtainable. For example 4-phenoxyphthalonitrile and 4-thiophenoxyphthalonitrile produce 2, 9, 16, 23-tetraphenoxyphthalocyanine and 2, 9, 16, 23- tetrathiophenoxyphthalocyanine as mixtures of isomers in 39% and 25% yield respectively. But in the past 2 decades Wohrle reported that substitution of alkoxide bases for strong bases such as 1, 8,-diazabicyclo[5.4.0]undec-7-ene (DBU) or 1,5-diazabicyclo[4.3.0]non-5-ene (DBN) gave the previously mentioned phthalocyanines in yields of 77% and 96% respectively. Introduction of these substituents alters the physical, chemical and electrochemical properties of the macrocycle [49,50].

1.6.2.6 Unsubstituted (Metal Free) Phthalocyanines (H₂Pcs)

These are phthalocyanines that have hydrogen in the inner cavity of the macrocycle. Linstead proposed a method for synthesizing H₂Pcs; phthalonitrile precursor or diiminoisoindoline is refluxed 2-N, N-dimethylaminoethanol, followed by dementallation via reacting the solution with dilute acids to remove the alkali metals from the solution to obtain H₂Pc [51,52].

1.6.2.7 Peripheral Substituents (β) and Non peripheral substituents (α)

Phthalocyanine chromophores that have that have alkylthio and alkoxy on the peripheral (2, 3, 9, 10, 16, 17, 23, 24) and non peripheral (1, 4, 8, 11, 15, 16, 22, 25) positions of the macrocyclic ring shown in Figure 1.4.
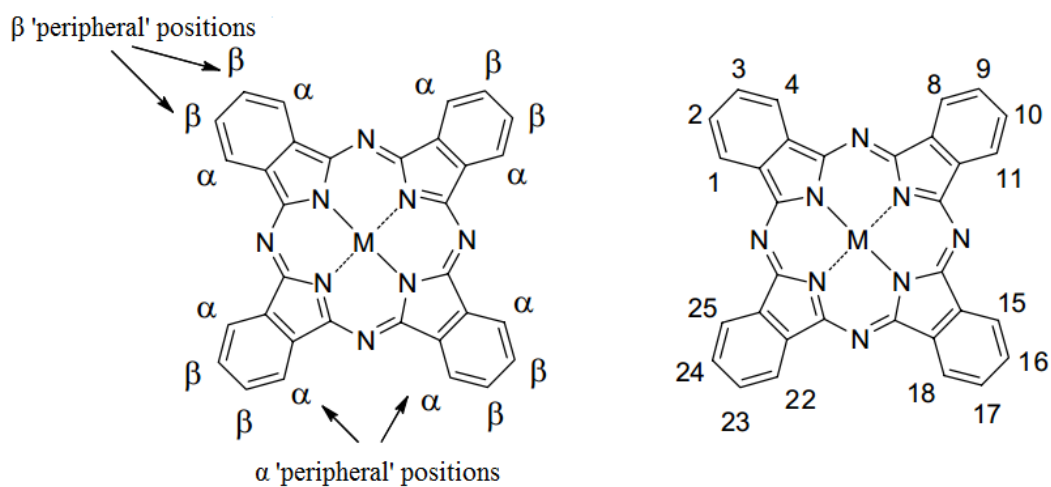
Figure 1.4: Substitution positions on the phthalocyanine molecule

1.6.2.8 Metallophthalocyanines (MPcs)

Pcs that have a metal atom (for example Cu, Co and Zn) located at the inner cavity of the macrocycle of the phthalocyanine are called metallophthalocyanines [37]. Phthalonitrile, phthalic anhydride, phthalimide and other precursors are metallated through various synthetic routes in the presents of the metal ion to produce MPcs [3,5,53]. Symmetrical change is controlled by the nature of the solvent used, central metal size, axial and ring substituents. Scheme 1.2 shows synthetic route for metallophthalocyanines.
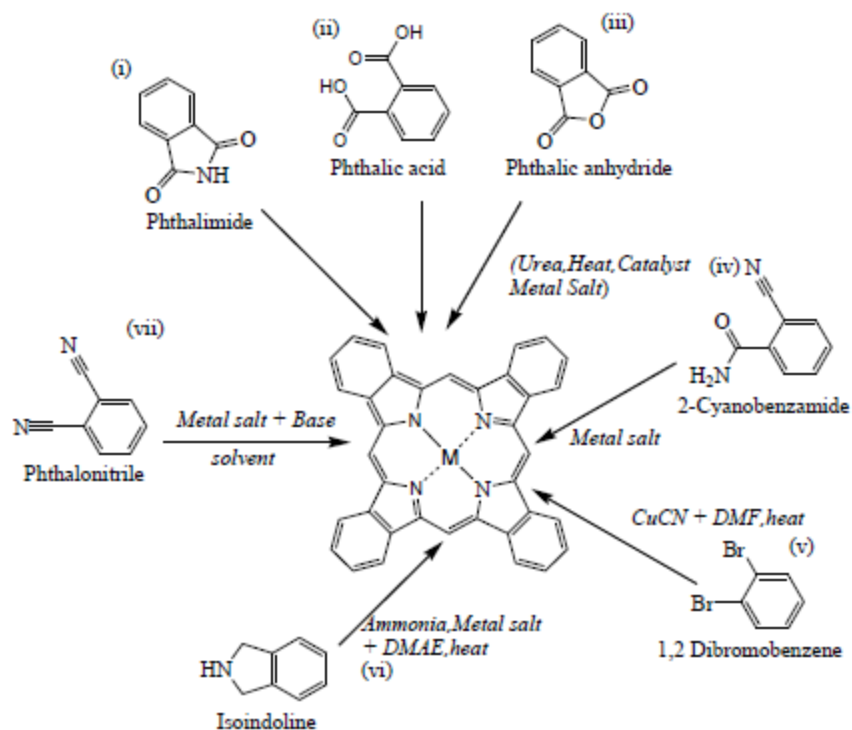
Scheme 1.2: General synthetic routes for metallated phthalocyanines.

1.6.3 Characterisation of synthesised complex

1.6.3.1 Infrared Spectroscopy

FTIR is an analytical technique used to confirm the structural changes during the synthesis of a complex by observing the appearance and disappearance of vibration band [54,55]. Infrared spectroscopy (IR) can be used for compound identification basing on the region of the electromagnetic spectrum. In this study for instance Pcs can be identified through the appearance of vibration frequencies of such as C-N, C-H and aromatic group, hence serves as a confirmation for the synthesis of Pc complex [56].

1.6.3.2 Ultraviolent-visible spectroscopy (UV-Vis)

This is a technique used for both qualitative and quantitative analysis basing on the basis of the characteristic absorption in the ultraviolet and visible light regions [57]. The UV-Vis of CoTCPc and N-GONS is best acknowledged through the use of a molecular orbital diagram in Figure 1.5.
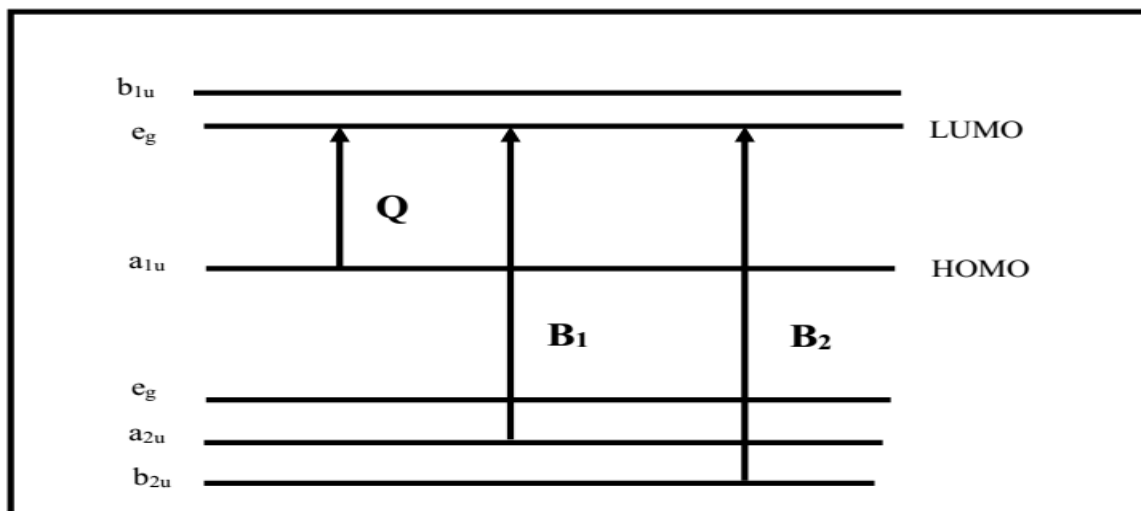
Figure 1.5: Molecular orbital diagram: Transitions of phthalocyanine that give rise to absorption bands [4].

Experimental and theoretical studies prove that the UV-Vis spectrum of Pcs is strongly dominated by $\pi - \pi^*$ transition in the strong Q-band (600 nm -750 nm) and broad B-band (300 nm - 450 nm). Gouterman et al. illustrates that the strong Q-band (600 nm – 750 nm) is associated with transitions from a_{1u} to e^*_g orbitals ($\pi - \pi^*$). The broad B band is related to transitions between a_{2u} and b_{1u} to e^*_g orbitals [39,40,58].

Dissolved Pcs often show solvatochromic effects. Dimerization of Pc molecules in solution causes a (reversible) band shift. Interaction with the solvent results in deformation of the Pc molecules alter the symmetry of the molecules and influences the absorption

spectra[4,37,41,19,59,60], for example causes the splitting of absorption bands in case of D_{2h} to C_{2V} transitions.

1.6.4 Electro-analytical techniques

1.6.4.1 Electrochemistry

Electrochemistry is a chemistry branch that focuses on interrelation of electrical and chemical effects. These involve measurement of electrical quantities such current, potential, or charge and relationship to chemical parameters [61]. Electro-chemistry deals with the study of chemical changes brought about by passing an electrical current and the generation of electrical energy by chemical reactions [62]. Vast applications have been found for analytical purposes using these electrical measurements.

The chemical measurements in a homogenous bulk solution occur at the electrode-solution interface. Different electro-analytical techniques are used to monitor such processes. These techniques differ in the type of analytical signal used. There are two major types of electrochemical sensors, namely potentiometric and voltammetric methods

- Potentiometric methods – in these methods no current passes between the electrode, and the concentration of the species in the electrochemical cell remain unchanged or static, hence why the method is sometimes called static [63].
- Voltammetric or amperometric methods – these are techniques that involve application of a linearly varying potential between a working electrode and a reference electrode in an electrochemical cell containing a high concentration of an indifferent electrolyte to make the solution conductive (supporting electrolyte) and an electroactive species. The current through the cell is continuously monitored and a plot of current against potential is

16

obtained and is known as a voltammograms [63,64]. This technique deal with the study of charge transfer at the electrode – solution interface [65]. During the process the analytes gain or lose an electron, hence gets reduced or oxidized respectively [61]. As a result these methods are applicable to any species that undergoes a redox reaction as the resultant current is a sign of the rate at which electrons move across the electron- solution interface.

This research focuses on voltammetric methods therefore it was important to firstly have an understanding of concepts voltammetry.

1.6.4.2 Voltammetric techniques

The value of the potential at an electrode cannot be directly known, thus it is the potential difference between the two electrodes that is measured. The electrode whose potential is a function of the analyte's concentration is called the working electrode (WE), while another electrode whose potential remains constant and against which other potentials can be measured is called the reference electrode (RE). The third electrode in the cell that completes the circuit is called the counter electrode (CE) [61,65]. Electrochemical analysis therefore employs three electrodes as shown in Figure 1.6. The potential is applied to the WE, changing its potential relative to the fixed potential of the reference electrode. The resulting current between the working and counter electrode is measured. Common examples of a counter electrode is platinum wire while that of a reference electrode are the Saturated calomel electrode (SCE) and as for this study Ag/AgCl electrode [64,66]. Examples working electrodes include mercury, platinum, gold, silver and carbon electrodes.
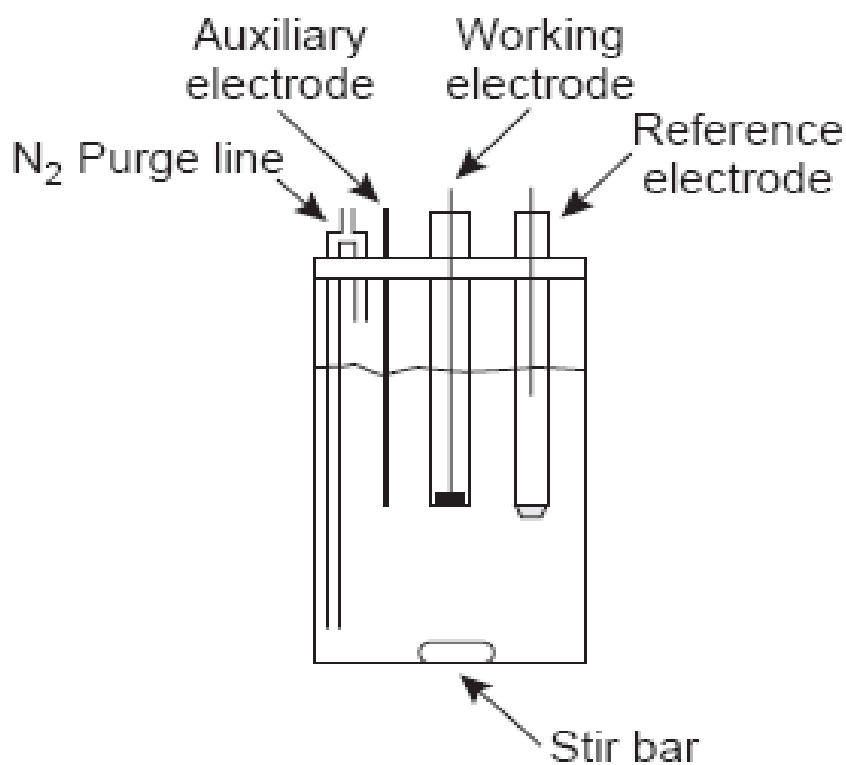
Figure 1.6: Systematic representation of a three electrode cell [66].

The current recorded will be comprised of two components; faradaic and non- faradaic currents. Faradic currents are currents in an electrochemical cell due to an oxidation and reduction reaction and it is that component of the overall charge that follows Faraday's laws. Thus linked to the sum of the electron- transfer reaction effect, which is proportional to the concentration of the analyte. This is achieved by monitoring the charge transfer during the redox process described as;

$$O + ne^- \longleftrightarrow R$$

where O and R are the oxidized and reduced forms of the redox couple, respectively. The measured current is normally more than the theoretical current.

The extra current is said to be non faradaic, as it does not follow Faraday's laws. The overall current observed is

$$L_{overall} = l_{faradaic} + l_{non\text{-}faradaic}$$

The non faradaic current can affect the sensitivity of electrochemical techniques, thus there should be minimized by careful selection of reagents, apparatus and experimental design.

1.6.4.3 Cyclic voltammetry (CV)

In cyclic voltammetry, the potential is scanned to more positive values, resulting in the following oxidation reaction for the species R

$$R \longleftrightarrow O + ne^-$$

When the potential reaches a predetermined switching potential, the direction of the scan reverses toward more negative potentials. Since the species O is generated on the forward scan, during the reverse scan it is reduced back to R.

$$O + ne^- \longleftrightarrow R$$

Cyclic voltammetry is carried out in an unstirred solution, hence the resulting cyclic voltammograms in Figure 1.7
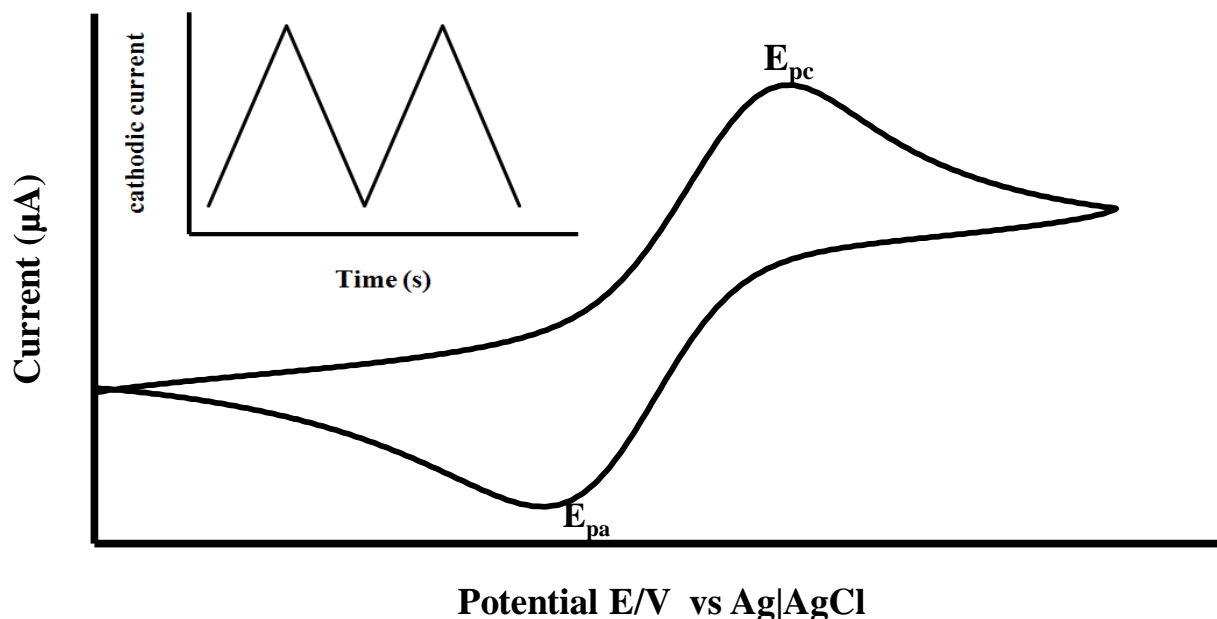
Figure 1.7: Potential against current for cyclic voltammetry. Inset: Waveform, Potential against time [65].

The peak current in cyclic voltammetry is given b the Randles - Sevcik Equation (1.1);

$$i_p = (2.69 \times 10^5)n^{\frac{3}{2}}A_{eff}D^{\frac{1}{2}}v^{\frac{1}{2}}C \qquad \text{Equation (1.1)}$$

where *n* is the number of electrons in the redox reaction, A_{eff} is the effective surface area of the working electrode, *D* is the diffusion coefficient for the electroactive species, *v* is the scan rate and *C* is the concentration of the electroactive species at the electrode [61].

For a well behaved system, the anodic and cathodic peak currents are equal, and the ratio i_{pa}/i_{pc} =1.00. The half-wave potential $E_{1/2}$ is the midway between the anodic and cathodic peak potentials, given by Equation (1.2);

$$E_{1/2} = \frac{E_{pa}+E_{pc}}{2} \qquad \text{Equation (1.2)}$$

Cyclic voltammetry is one of the electrochemical methods that are convenient to mechanisms and kinetics. It is also a powerful tool for studying redox reactions in aqueous and organic solutions, surface deposition and adsorption. CV is usually the first experiment performed in electro-analysis to provide information on the reversibility, kinetics, and oxidation and reduction potentials of a system [67]. Once there is a proper mechanistic understanding of the system, other methods are usually better suited for the precise evaluation of parameters, for example concentration.

The peak separation of a reversible process is given by Equation (1.3);

$$\Delta E_p = E_{pa} - E_{Pc} = \frac{0.059}{n} \qquad\qquad \text{Equation (1.3)}$$

In reversible process ΔE is always greater than 0.059/n V, while for an irreversible process only one peak will be observed on one of the potential scans. Peak separation (ΔE) can be used to calculate the number of electron involved in the system. For systems that have a poor electron exchange system, the peaks are widely separated and reduced in size.

1.6.4.4 Differential Pulse Voltammetry (DPV)

Differential pulse voltammetry is a more sensitive method compared to cyclic voltammetry. According to Wang (2001) detection limits can be lowered to nano-molar range by increasing the ratio between the faradaic and non faradaic currents [61]. The method uses a series of potential pulses characterized by cycle of time (t), a pulse time of t_p, a potential pulse of ΔE_p and a potential step per cycle of $\Delta E_{p\,S}$ in Figure 1.8(A). Typical experimental conditions for DPV are t = 1 s, tp = 50 ms, ΔE_p = 50 mV, $\Delta E_{p\,S}$ = 2 mV. The current is measured twice, for approximately

17 ms before the forward pulse and for 17 ms before the reverse pulse. The difference between the two gives rise to a peak shaped voltammogram in Figure 1.8 (B) [61,62].
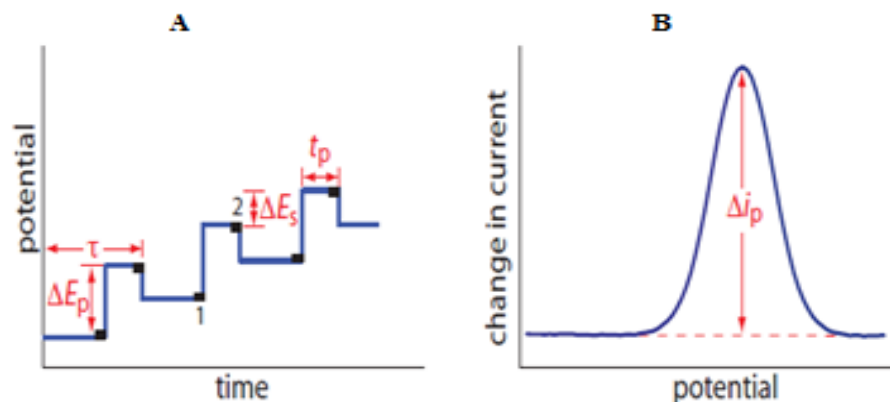
Figure 1.8: A. Typical Waveform, Potential against time; B. Potential against current for Differential Pulse voltammetry [61].

1.6.5 Types of Electrodes.

Electrodes or electrode materials are metals or substances used as the makeup of electrical components ad are used to make contact with a nonmetallic part of a circuit. They are the component in a system through which an electrical current is transferred [68] and they are sometimes referred to as substrates. Examples include platinum (Pt), gold (Au), carbon, or semi-conductor (SnO_2) [61]. The electrode materials must have some basic properties such as good mechanical and chemical stability.

The material of the working electrode influences performance of voltammetric experiments. The working electrode must provide high signal noise ratio and good reproducibility. This implies that a number of factors are considered before an electrode is chosen for any experiment. These include redox behavior of the target analyte, background current over the potential region

required, electrical conductivity, mechanical properties, potential window, availability, cost, surface reproducibility and toxicity [16,13,11].

1.6.5.1 Carbon electrodes

Carbon is a very important widely used electrode material with advantages such as low cost, low residual currents, chemical inertness, easy modification, great versatility and broad potential window [69,70]. Properties such as good conductivity, resistance to environmental and chemical hazards make carbon suitable for electrochemical detection. To enhance and extend application of these various carbon forms in electrochemical detection systems, the modification of carbon surface is essential [71]. The common carbon based electrodes are glassy carbon electrode (GCE), carbon fibres electrodes and carbon paste electrodes. Amongst these electrodes glassy carbon electrode was chosen for this research.

1.6.5.2 Glassy carbon electrode (GCE)

Glassy carbon is a conductive form of carbon made by pyrolysing carbon or graphite [65]. It is a form of carbon that is extremely hard and highly conductive to electrons, and is thus a good choice for fabricating inert electrodes [72]. This electrode is the most widely used electrode of all carbon based electrodes. A large number of electrochemical publications in which GCE is used mostly with some form of modification, are seen due to its popularity. These include its use in heavy metal analysis [73–75], biological compounds, nitrates [7,13,76] and other important compounds such as electro-catalytic oxidation of methanol [77], pentachlorophenol and many other analyses.

1.6.5.3 Electrode modification

Electrodes do not possess selectivity, except that which is due to variations of the imposed potential. Therefore electrode modification forms a major part of electrochemical research. The modification of electrodes can be described as the process whereby the electrode is purposely covered with an adsorbed layer or film to produce an electrode suited for particular function. This is done to improve the electron transfer kinetics by using electron transfer mediators such as redox active metal nanoparticles, since bare electrodes usually have slow electron transfer behavior [78]. The properties of the modified electrode are usually different from those of the unmodified such as the electron transfer rate [79] and the electroactive surface area. Modified electrodes, therefore usually show a decrease in the activation over-potential and hence effectively speed up the reaction, thus reducing interferences and results in lower limits of detection [80] in addition to selectivity and sensitivity.

Modification of electrodes can be accomplished in various ways such as covalent attachment of a monolayer, irreversible adsorption and coating the electrode with a film of polymer or other material [81]. The type of modification used is based mainly on the feasible function. For this work, GCE was used as an electroanalytical sensor thus modification was directed towards selectivity and lower detection limits for the nitrite ions. Nanomaterials (CoTCPc and N-GONS) were used for modification of the GCE by drop-drying technique.

The drop-dry method involves placing a drop of the modifier on the electrode surface and then letting it dry [82]. The major advantage of this approach is that the coverage is immediately known from the solution concentration and droplet volume [55]. Other modification techniques include dip-drying, spin coating, electrochemical polymerization and electrodeposition. The main aim of electrode modification is usually to increase catalytic effect towards a certain

24

analyte. Therefore electrocatalysis at a modified electrode usually proceeds at a lower overpotential than it would occur at the bare electrode.

Nanomaterials have a good reputation for their high surface areas and interesting chemical properties such as catalysis hence their use in electrocatalysis.

1.6.5.4 Nanoparticles (NPs) modified electrodes

In this modernizing technical world nanoparticles have attracted attention owing to their low cost and unique properties. There applicability includes uses in catalysis, optics, bioelectronics and biosensors. Some of the properties that make NPs unique include their electrical, optical, mechanical, magnetic and catalytic properties and also they have a high surface area to volume ratio [83]. Owing to their extra ordinary physical and chemical properties especially their catalytic nature, NPs have been employed in many electrochemical applications.

Glassy carbon electrodes (GCE) can host metal nanoparticles or as composite with other materials as this has been accomplished in a number of electrochemical studies. For this study CoTCPc and N-GONS are used for modification.

1.7 Electrode characterisation

The use of a modified electrode requires the use of physical and electrochemical characterisation.

1.7.1 Physical characterisation techniques for nanomaterials

When nanomaterials are synthesised, they should be followed by characterisation to get information on their size, charge, shape and composition [84]. The properties of a material can be greatly influenced by particle size if it is of concern in nanotechnology. Some of the techniques used to study the size and arrangement properties include Scanning Electron Microscopy (SEM), Tunneling Electron Microscopy (TEM) and X-Ray Diffraction (XRD)

1.7.1.1 Powder X-Ray Diffraction

X-ray scattering has for many years been used to study the long range order of the atomic arrangement in crystals and is now also used in the characterisation of nanomaterials. The atomic structure influences the pattern, intensity, position, shape of the peaks in XRD [84]. This technique is not element specific thus the diffraction pattern of unknown samples must be compared to those of reference compounds from the database. Information regarding the size of nanoparticles may also be derived from the XRD pattern as the size strongly affects the peak width [84]. It also gives information about the crystalline nature of compound and the difference in the d-spacing.

1.7.1.2 Scanning Electron Microscopy (SEM)

This technique gives information about the size and morphology of nanoparticles. This is obtained by using a finely focused beam of electrons to scan sample surface. The interaction between the electron beam and solid surface result in a number of elastic and inelastic scattering processes [84]. During scanning the incident electrons are completely backscattered, remerging from the surface of the surface. Since the scattering angle is strongly dependent on the atomic number of the nucleus involved, the primary electrons arriving at a given detector position can be used to yield images containing both topology and compositional information [84]. This therefore makes the technique useful for the morphological characterisation of nanoparticles.

1.7.2 Electrochemical characterisation.

For any electrode substrate there is a need to electrochemically probe in order to ascertain whether that electrode can be used for any electrochemical study. This is usually done by performing a number of electrochemical experiments (such as CV and sometime electrochemical impedance spectroscopy, EIS) in some redox systems.

There are a number of redox systems that been have used to describe and explain the electron-transfer kinetics on the carbon – electrode based on their electrochemical reversibility. These can be classified into quasi-reversible inorganic systems and quasi-reversible organic systems [85]. The $[Fe\ (CN)_6]^{3-/4-}$ redox probe has been extensively studied to benchmark various electrodes while electron-transfer kinetics on glassy carbon electrodes (GCE) have also been extensively investigated. Other redox probe are $[Ru\ (NH_3)_6]^{2+/3+}$ (which is positive while $[Fe\ (CN)_6]^{3-/4-}$ is negative) and ferrocene (an organic probe).

1.7.2.1 Electrochemical impedance spectroscopy (EIS)

This technique is applied for characterisation of modified electrodes to study the properties of the interface [86]. The technique is used to investigate the dynamics o bound or mobile charge in the bulk region of any kind of solid or liquid material. EIS is the ratio of the alternating potential and the alternating current signal. The technique is favoured for assessing probe surface-confined species due to advantages which include; potential to adapt for various applications, the ability to obtain accurate and reproducible measurement and rapid acquisition of such as charge or electron transfer at the electrode-film interface [87].
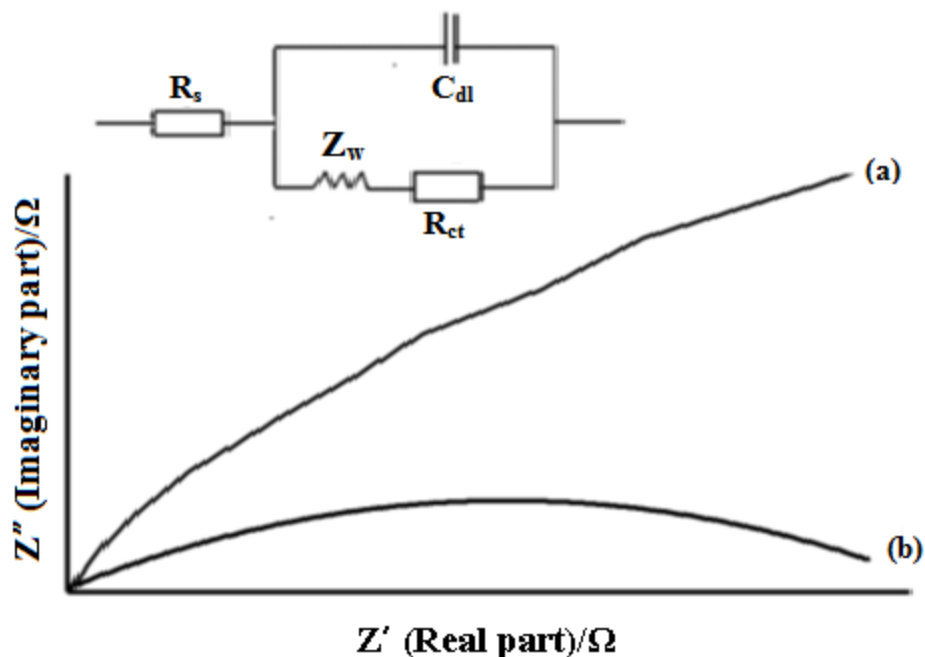
Figure 1.9: Nyquist plot of imaginary impedance against real impedance. Inset: A typical representation of Randles equivalent circuit for an electrochemical system [88].

A Nyquist plot is a typical plot that can be obtained, this consist of imaginary impedance (Z imaginary) versus the real impedance (Z real). It includes a semicircle at high frequencies and linear portions at low frequencies. The diameter of the circle is equivalent to the electron transfer resistance (R_{ct}), which monitors the electron transfer kinetics of the redox electrode at the electrode interface [89]. The plots of the bare and modified electrodes are compared generally the bare electrode (Fig: 1.9 (a)), is known to display an almost linear curve due to mass diffusional limiting electron transfer processes. Considering the modified electrode (Fig: 1.9(b)) the Nyquist plot displays a characteristic semi-circle which is fitted by the Randles equivalent circuit (R_{ct}) (Fig: 1.9). This is known to be due to nature and thickness of the surface of the modified electrode. The Randles equivalent circuit (Fig: 1.9 insert) consist of R_s (the resistance

of the electrolyte), in series connection with parallel elements of C_{dl} (double layer capacitance), R_{ct} (resistance to charge transfer) and Z_w (Warbung impedance) [86].

1.8 Summary of the aims of the research

Electrodes do not posses selectivity, except that which is due to variation of the imposed potential. Therefore electrode modification forms a major part of electrochemical research whereby nanomaterials are being used as modifiers. Nanotechnology is now subject of major concern in terms electrochemistry to produce an electrode suited for a particular function. Chemical or physical coupling of nanoparticles such as N-GONS with CoTCPc can improve selectivity and electron transfer kinetics, since bare glassy carbon electrodes usually have sluggish electron transfer behavior. Based on these known attractive characteristics, the research is being pursued.

CHAPTER 2

EXPERIMENTAL

2.0 Introduction

This chapter presents the experimental procedures followed in order to accomplish the set objectives. The experimental procedures were done to synthesis CoTCPc, N-GONS was kindly provided by my supervisor Mr Shumba. Then their catalytic properties as BGCE modifiers on the determination of nitrites was evaluated using cyclic voltammetry, impedance spectroscopy (EIS) and differential pulse voltammetry (DPV). Factors such as pH and scan rate were investigated to evaluate the applicability of the best electrode in the electrocatalytic oxidation of nitrite.

2.1 Chemicals and reagents

All the chemicals which were used in this study were of analytical grade and were used without further purification. Trimellitic acid anhydride ($C_9H_4O_5$) from Aldrich chemistry; cobalt (II) chloride ($CoCl_2.6H_2O$) and nitrobenzene ($C_6H_5NO_2$) from Alpha Chemika; ammonium molybdate (($NH_4)_2MoO_4$) from Glass world; sodium nitrite ($NaNO_2$) from Minema; phosphoric acid (H_3PO_4), potassium ferrocyanide ($K_3[Fe(CN)_6]$); ammonium chloride (NH_4Cl), sodium chloride ($NaCl$), di- Sodium hydrogen phosphate (Na_2HPO_4) and potassium dihydrogen phosphate KH_2PO_4 from Merck Chemicals; urea ($CO(NH_2)_2$) from Radchem. Dimethyl sulfoxide (C_2H_6OS) and methanol (CH_3OH) from Associated Chemical Enterprises. Ethanol (C_2H_5OH) from Cosmo chemicals; sodium hydroxide ($NaOH$), potassium chloride (KCl) and hydrochloric acid (HCl) from Skylabs. Distilled water was used to prepare all solutions. A stock

solution of K_3 [Fe (CN) $_6$] in 1 M KCl was prepared in 1000 ml; phosphate buffers were prepared from Na_2HPO_4 and KH_2PO_4.

2.2 Equipment

Reagents were weighed using an Analytical Balance Model JJ224BC. UV- Vis spectroscopy was used for characterisation on the Shimadzu UV-1700 spectrophotometer with Pharmaspec software. FTIR spectra were obtained using Thermo-scientific Model equipped with OMNIC software. Sonicator model KQ-250B was used for agitation of samples. All electrochemical experiments were performed using Auto potentiostat PGSTAT302N equipped with NOVA version 1.10 software and encompassed with a three electrochemical cell comprising of a glassy carbon electrode (GCE), platinum wire counter and Ag|AgCl reference electrode.

2.3 Synthesis of cobalt tetracarboxy-phthalocyanine (CoTCPc)
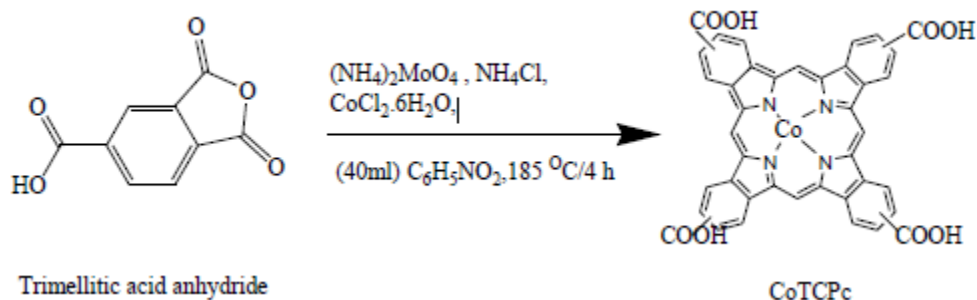
Figure 2.1: Synthesis of Cobalt tetracarboxy-phthalocyanine (CoTCPc) [52]

Trimellitic acid anhydride (4.79 g,), cobalt (II) chloride (3.71 g), ammonium chloride (0.27 g), ammonium molybdate (0.59 g), and urea (15 g) were mixed and finely ground. The mixture was then added to 40 ml of nitrobenzene and was heated under reflux at 160 ^{0}C - 190 ^{0}C for 4 h. A dark coloured solid was formed in solution and this was filtered off and washed several times with methanol. Then the solid was Soxhlet extracted for 12 h to further remove any nitrobenzene

left and then was dried overnight at 70 ^{0}C to form the amide complex, which was boiled with 275 ml of 1 M HCl and excess NaCl. The solution was neutralized by 1 M NaOH then separation of the solid was done by vacuum filtration and to the resultant sodium salt solution, 1 M HCl was added to precipitate the tetracarboxyl-complex. The solution was then filtered and the resultant dark blue/green complex was dried at 70 ^{0}C in an oven and then was stored in a desiccator prior to further procedures.

2.3 Characterisation of CoTCPc, N-GONS and mixture.

2.3.1 Fourier Transfer Infrared Spectroscopy (FTIR)

FTIR was used to characterize all the samples in liquid state. The IR spectra for all samples were obtained by using solutions and suspension of analytes in DMSO.

2.3.2 Ultra-Violent Spectroscopy (UV-Vis)

The UV-Vis electronic absorption spectra were obtained by using solutions and suspension of analytes in DMSO, using a 1 mm quartz cuvette.

2.4 Electrochemical methods

2.4.1 Preparation of electrode modifiers

Masses of 0.1 g of the synthesised CoTCPc and 0.1 g N-GONS were both dissolved in 50 ml DMSO and a mixture of the two was prepared from 0.1 g of each complex and dissolved in 100 ml DMSO and these solutions were ultra-sonicated for 30 minutes.

2.4.2 Chemical modification of electrodes

Before modification the BGCE was carefully polished with alumina paste on Buehler felt pads and then was ultrasonically cleaned in ethanol for 5 minutes. Then rinsed with distilled water and

was air dried before each modification. The cleaned BGCE was modified by drop and dry method by applying 2 µL of each of the modifiers. The dry GCE was then modified with CoTCPc, N-GONS and CoTCPc and N-GONS mixture.

Table 2.1: Working electrodes used in this research.

Electrode Modifier	Electrode Designation
Bare Glassy Carbon.	BGCE
Cobalt tetracarboxyl-phthalocyanine.	CoTCPc-GCE
Nitrogen doped graphene oxide nanosheets.	N-GONS-GCE
Cobalt tetracarboxyl-phthalocyanine and Nitrogen doped graphene oxide nanosheets mixture	CoTCPc/N-GONS-GCE

2.5 Phosphate buffer

Phosphate buffer solution was prepared by mixing stock solution of 0.1 M KH_2PO_4 and 0.1 M Na_2HPO4 and adjusting the pH either with 0.1 M NaOH or 0.1 M H_3PO_4

2.6 Sodium nitrite analysis

A volume of 1 mM sodium nitrite was prepared by dissolving 0.0345 g in phosphate pH 7 buffer and diluted to 500 ml.

RESULTS AND DISCUSSION

3.0 Introduction

This chapter presents and discuses detailed research findings.

3.1 Characterisation

Synthesised CoTCPc, N-GONS and the mixture were characterized by FTIR spectroscopy and UV-Vis spectroscopy. FTIR was used to verify the available functional groups and UV-Vis spectroscopy to confirm the characteristic absorption spectra of the phthalocyanine and effect of mixing with N-GONS on the Q band.

3.1.1 Fourier Transfer Infrared Spectroscopy (FTIR)
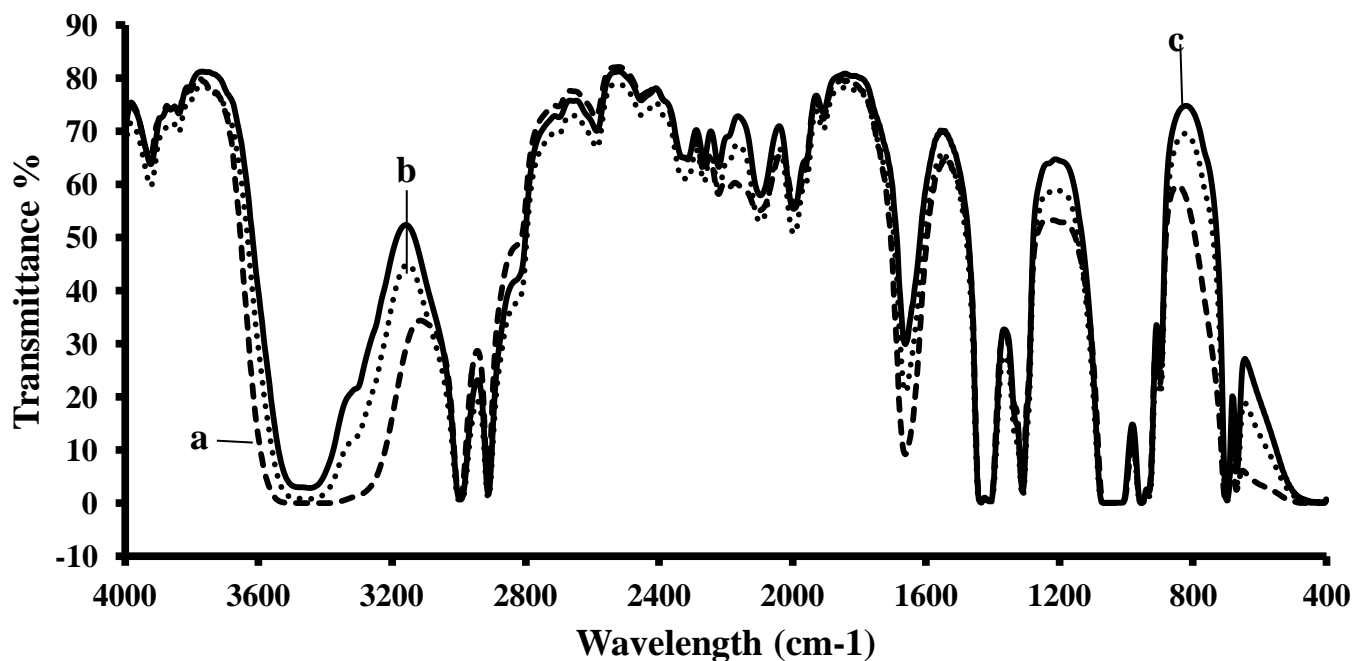
Figure 3.1: FTIR spectrum for: (a) CoTCPc, (b) N-GONS and (c) CoTCPc/N-GONS composite.

FTIR spectra of all the three complexes were recorded in the fundamental region 4000–400 cm^{-1} (Fig 3.1) by analysis of liquid samples of the complexes in DMSO. Peaks at 699.39-701, 873.34-888, 911- 954.90, 1087-1096 and 1121-1165 cm^{-1} are observed for CoTCPc (fig 3.1(a)) which may be assigned to phthalocyanine skeletal vibrations [80,90]. The vibration band at 1662.42 may be assigned to C=O carbonyl of the tetra carboxylic acid groups. Also broad O-H stretch from 3403.80-3270 cm^{-1} was noticed. The peaks at 1312.36 and 1095.32 cm^{-1} are typical stretches of C-O [56].

The FTIR spectra of N-GONS (Fig 3.1(b)) displayed peaks at 1662.36 and 1435.36 cm^{-1} corresponding to the C=O stretching vibration peak and aromatic C=C stretching peak. Also bands at 2221.86 and 1160 cm^{-1} can be assigned to CN triple bond and C-N stretching [91].

The FTIR of the mixed complexes (Fig 3.1(c)) shows no significant bathochromic effect as the peaks show no red shifting.

3.1.2 UV-Vis Spectroscopy
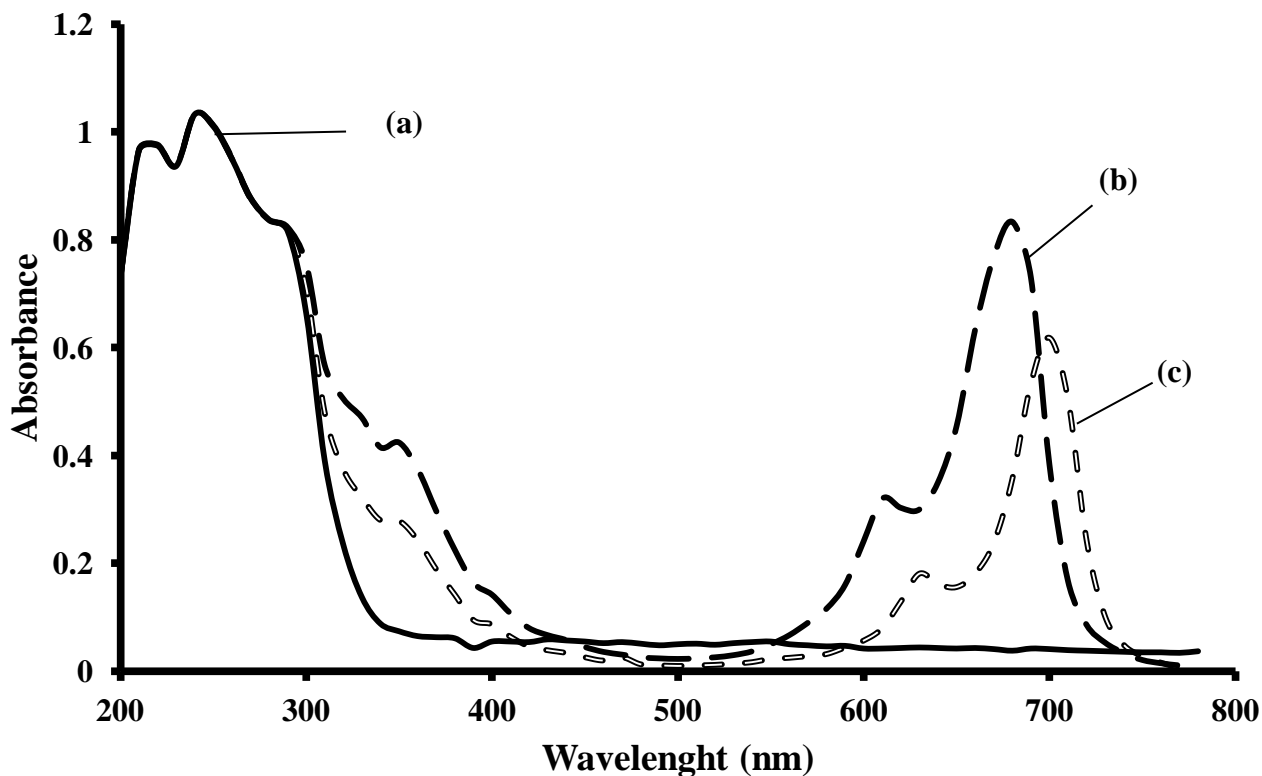
Figure 3.2: Electronic absorption spectra of: (a) N-GONS, (b) CoTCPc and CoTCPc/N-GONS mixture. Solvent dimethyl sulphoxide (DMSO).

The UV-Visible spectra of N-GONS (Fig. 3.2 (a)), bands appeared at 210 nm and 230 nm. The bands can be assigned to $\pi - \pi^*$ transition of C=C [22,92,93] and $n - \pi^*$ of the carbonyl groups [22,58], due to the transition from the highest occupied molecular orbital (HOMO) to the lowest unoccupied molecular orbital (LUMO). The spectra for CoTCPc (Fig. 3.2 (b)) had B-band at 610 nm and a strong absorption peak (Q-band) at 680 nm. The Q-band is attributed to allowed $\pi - \pi^*$ transition [41]. The UV-Visible spectra of CoTCPc/N-GONS mixture (Fig. 3.2 (c)) showed a B- band at 630 nm and a red shifted Q-band at 00 nm, indicating that CoTCPc interacted with N-GONS. The red shifting (Bathochromic) shift due to the electron transfer from

electron rich N-GONS to phthalocyanine ring, thus lowering the gap between the highest occupied molecular orbital (HOMO) and lowest unoccupied molecular orbital (LUMO) [29,37,94]. According to literature this electron transfer results in the formation of $\pi - \pi$ stacking interaction between graphene sheets and CoTCPc [16,42,69].

3.2 Electrochemical characterisations

3.2.1 Voltammetric studies in 5 mM K_3 [Fe (CN) $_6$] (in 1 M KCl solution)

All electrodes were scanned in 5 mM K_3 [Fe (CN) $_6$] (in 1 M KCl) and the obtained cyclic voltammograms and ΔE_p values are shown in Fig 3.3 and Table 3.1 respectively.
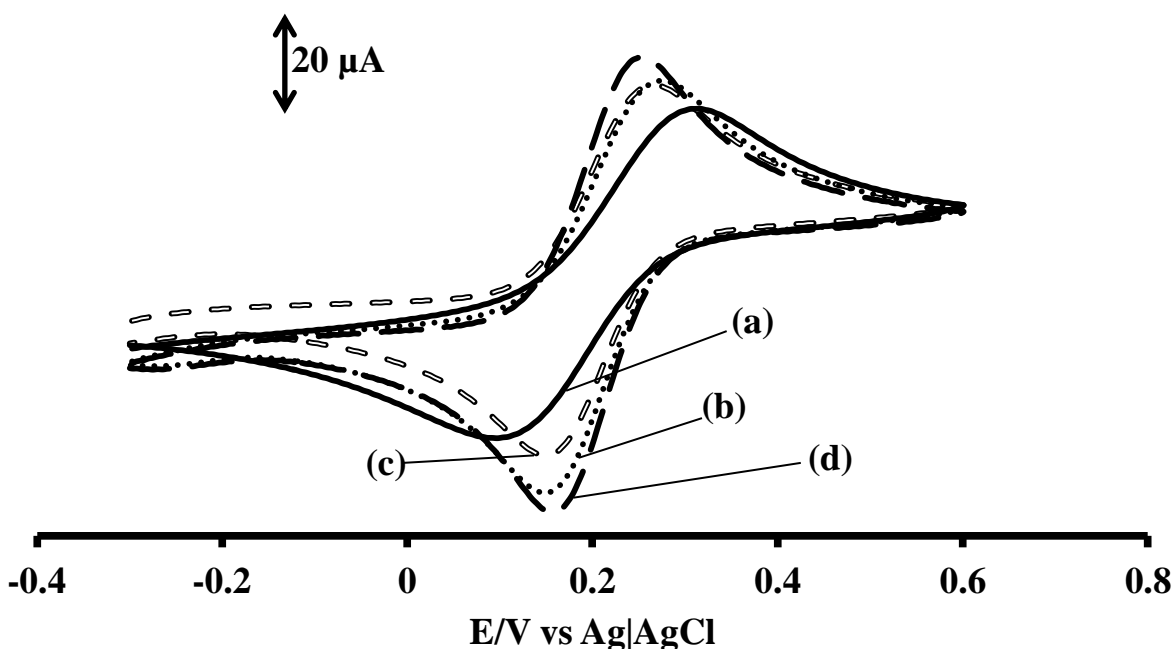
Figure 3.3: Cyclic voltammograms for: (a) BGCE, (b) CoTCPc-GCE, (c) N-GONS-GCE and (d) CoTCPc/N-GONS-GCE in 5 mM K_3[Fe (CN) $_6$] (in 1 M KCl). Scan rate =100 mV/s.

Table 3.1: ΔE_p values of all working electrodes.

Electrode Modifier	Δ Ep values/V
BGCE	0.21
CoTCPc-GCE	0.13
N-GONS-GCE	0.11
CoTCPc/N-GONS-GCE	0.09

The different electrodes gave peak potential differences with the following trend: CoTCPc/N-GONS-GCE < N-GONS-GCE < CoTCPc-GCE < BGCE (as shown in Table 3.1).

The CoTCPc/N-GONS-GCE displayed excellent electron-transfer rate among all the electrodes. The above trend displays the advantage of combining a metallophthalocyanine and the nitrogen doped graphene complex compared to the bare electrode as the phthalocyanine creates a suitable microenvironment for the electroactive graphene and thus increase the electrochemical activity [16,31,43]. The ΔE_p values decrease from bare to CoTCPc-GCE, is due to the improved flow of electrons on the surface of the electrode due to pie electrons in the Pc [29].

From CoTCPc-GCE to N-GONS-GCE, is due to the unique nanostructure, the covalent interactions between N and graphene, the conductivity and high surface area which reduce the electron transfer enhancing better current flow.

From N-GONS-GCE to CoTCPc/N-GONS-GCE, mixing the MPc with graphene oxide nanosheets proved to have synergistic effect. This is due to the combined properties of the two complexes, especially due to nitrogen doped graphene oxide nanosheets which have superb

characteristics of chemical stability, high electrical conductivity and larger surface area [11,15,18].

3.2.2 Surface area determination

The surface area of the modified GCE was determined in 5 mM K_3 [Fe (CN) $_6$] in (1 M KCl), by applying the Randles - Sevcik Equation (3.1) [25]

$$i_p = (2.69 \times 10^5)n^{\frac{3}{2}}AD^{\frac{1}{2}}v^{\frac{1}{2}}C \tag{3.1}$$

where i_p is the peak current, n is equal to the number of electrons transferred at the surface of the electrode,

$$Fe(CN)_6^{3-} + e^- \rightarrow Fe(CN)_6^{4-} \tag{3.2}$$

From Equation (3.2), n is equal to 1, D is the diffusion coefficient of the analyte in solution i.e. $7.6 \times 10^{-6} cm^2 s^{-1}$ and C is the concentration in mol/cm^3, A_{eff} is the effective surface area and

v is the scan rate (V/s). From Equation (1), i_p is proportional to $v^{\frac{1}{2}}$ and produces a linear plot with slope m, given by the Equation (3.3)

$$m = (2.69 \times 10^5)n^{3/2}A_{eff}D^{1/2}C \tag{3.3}$$

Scan rate studies were done from 100 mVs^{-1} – 350 mVs^{-1}. Figure 2 shows the obtained voltammograms at different scan rates and a plot of i_p vs $v^{1/2}$ is shown as an insert. The plot showed a linear relationship with a R^2 value of 0.9906.
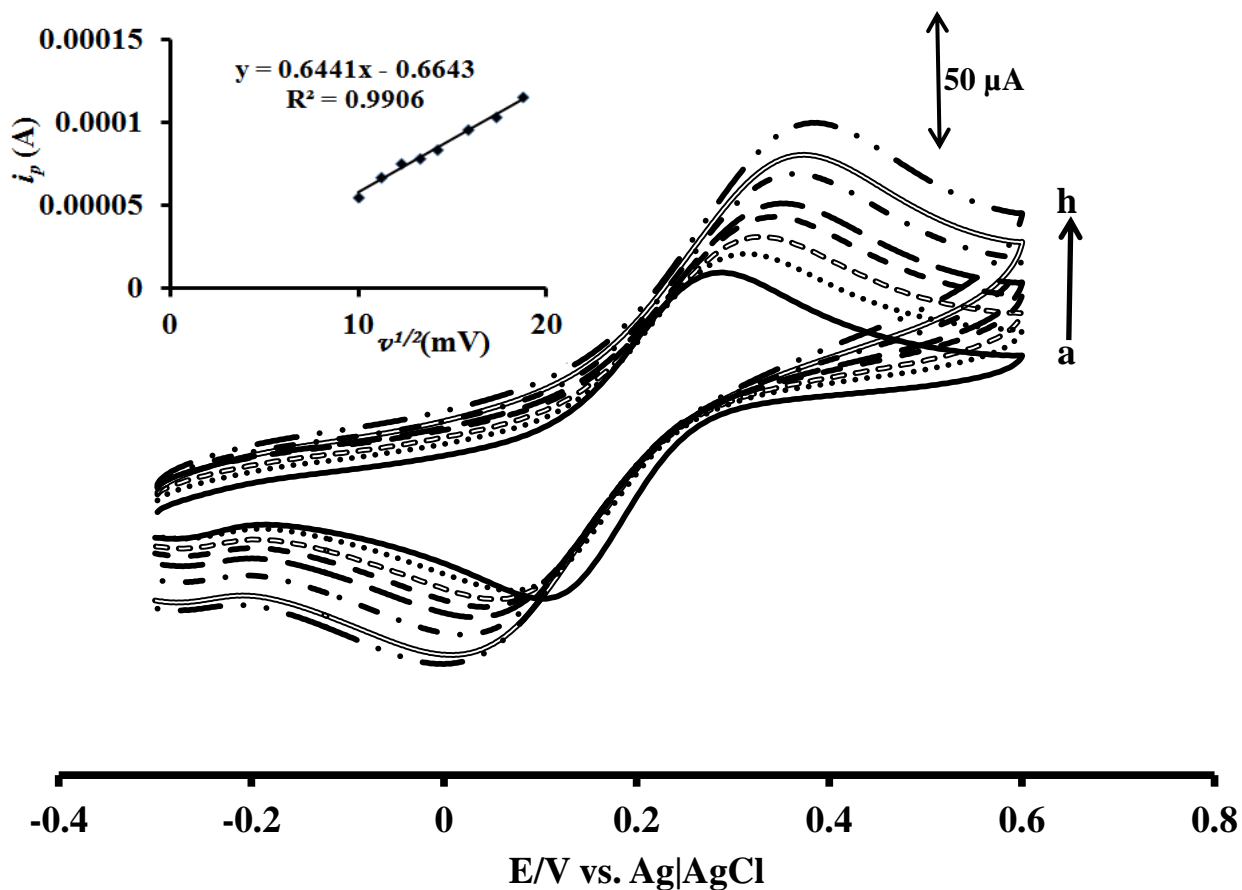
Figure 3.4: Effect of scan rate on peak potentials and currents (a) 100 mV/s, (b) 125 mV/s, (c) 150 mV/s, (d) 175 mV/s, (e) 200 mV/s, (f) 250 mV/s, (g) 300 mV/s and (h) 350 mV/s, on CoTCPc/N-GONS-GCE in 5 mM $K_3[Fe (CN)_6]$ (in 1 M KCl). Inset: Plot of peak current versus root of scan rate

Using Equation (3.3), the effective surface area of CoTCPc/N-GONS-GCE was found to be 0.174 cm^2. Comparing to the known surface area of BGCE of 0.0712 cm^2, the ratio was 2:1 respectively. This indicates that the modified electrode provided a large surface area for electro catalysis than the BGCE.

3.2.3 pH studies in phosphate buffer
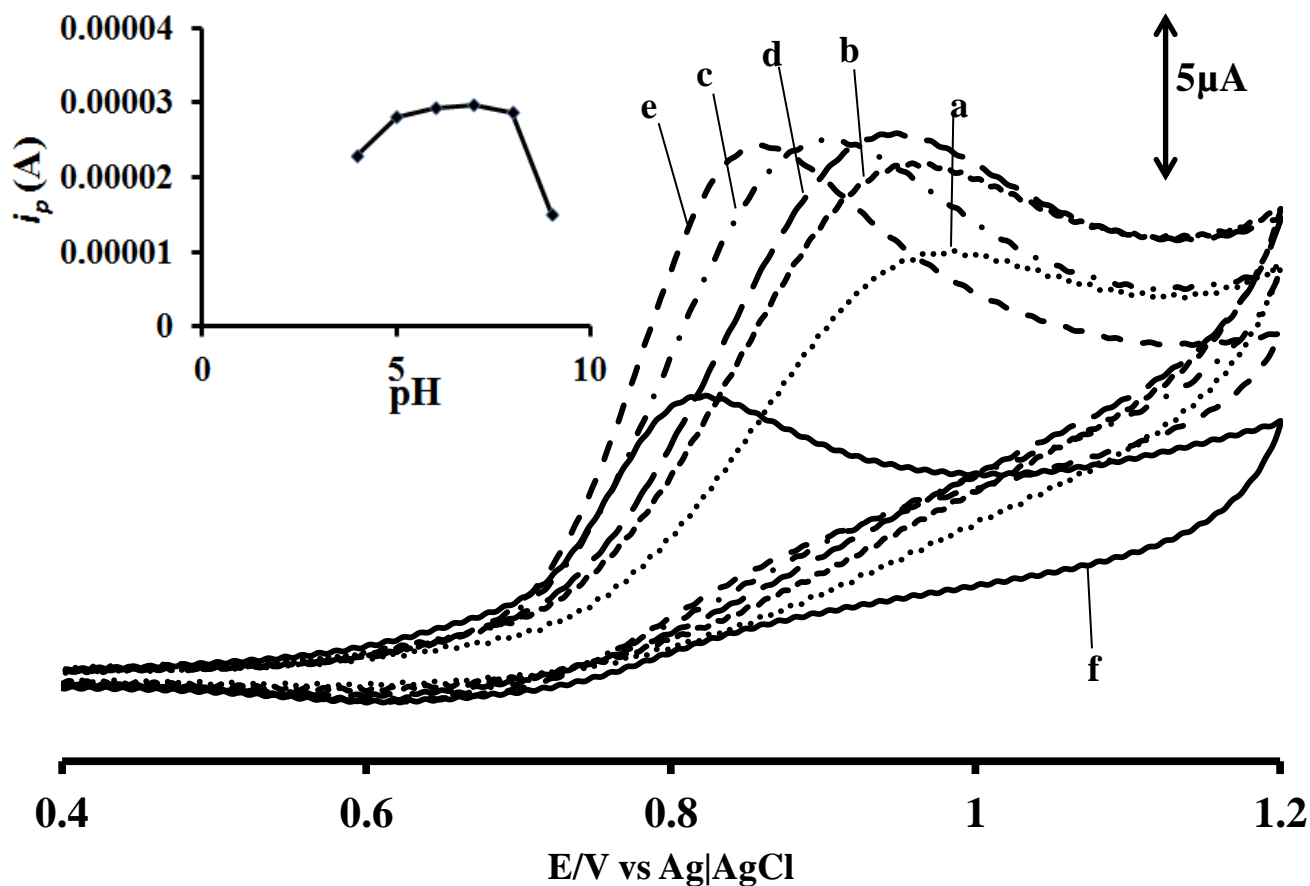
Figure 3.5: pH studies for CoTCPc/N-GONS in 1 mM sodium nitrite, from pH 4 to pH 9 (a-f) respectively. Insert: Plot of current against pH. Scan rate = 50 mV/s

pH was varied from 4 to 9 and peak potential and current for each pH were noted. Maximum peak current was observed at pH 7, but pH 6 was chosen as the optimum pH since it has a lower peak potential. The plot of peak current against pH also displays that the variation in peak currents for pH 5, 6 and 7 are very small and oxidation of sodium nitrite occurs at a lower peak potential at pH 6 (Figure 3.5 inset).
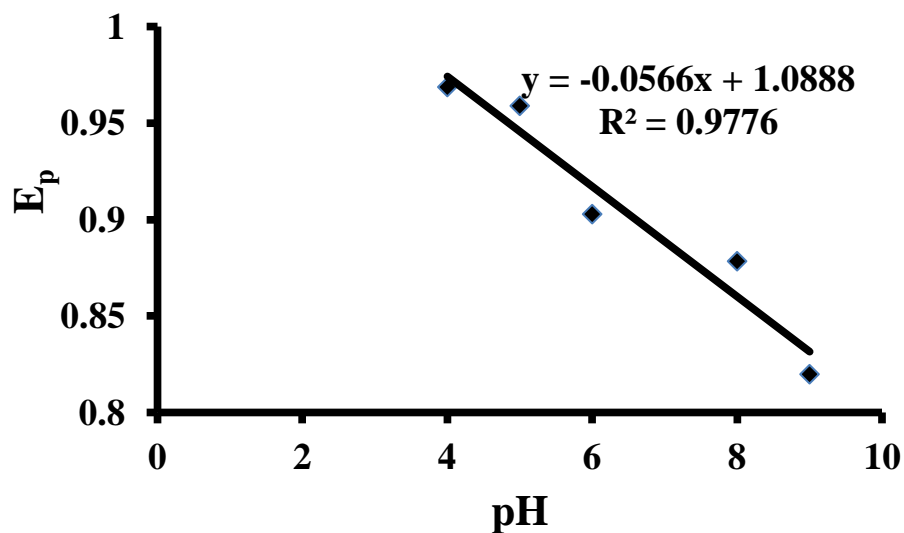
Figure 3.6: Plot of peak potential against pH

The plot of E_p against pH had a correlational value of 0.9776 and a slope of -0.0494, which proved that equal number of protons and electrons participated in the reaction [31]. The plot proves that the electrocatalytic oxidation of sodium nitrite is a one electron transfer process as indicated by the slope value obtained which was close to the actual slope value for a single electron transfer process which is -0.05916 [95].

3.2.4 Comparative studies in pH 6
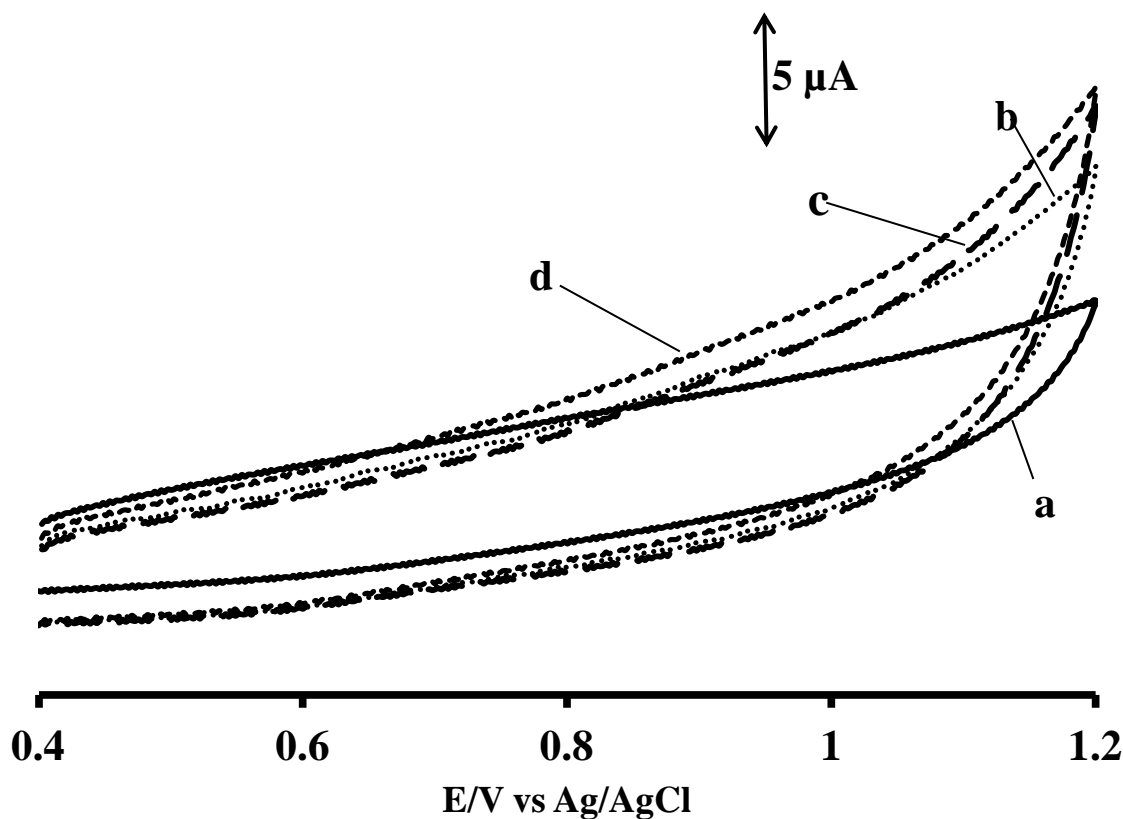
Figure 3.7: Cyclic voltammograms for: (a) BGCE, (b) N-GONS-GCE, (c) CoTCPc-GCE and (d) CoTCPc/N-GONS-GCE all in pH 6 phosphate buffer. Scan rate= 50 mV/s.

Electrodes (c) and (d) showed broad peaks at 0.86 V which were attributed by the oxidation between cobalt and the phthalocyanine ring ($Co^{III}Pc^{-1}|Co^{III}Pc^{-2}$) [95].

3.2.5 Surface Coverage

Surface coverage is defined as the thin film of modifier deposited on the electrode surface and it is calculated according to equation (3.4) [35,79].

$$i_{pa} = \frac{n^2 F^2 A \Gamma v}{4RT} \qquad (3.4)$$

where n is the number of electrons involved in the reaction, F is the faraday constant which is equal to 9.6487 C/mol, A is the effective surface area of the electrode, and Γ is the surface coverage in mol cm^{-2}, v is the scan rate, R is the gas constant (8.314 kJ/mol) and T is the temperature in Kelvins.
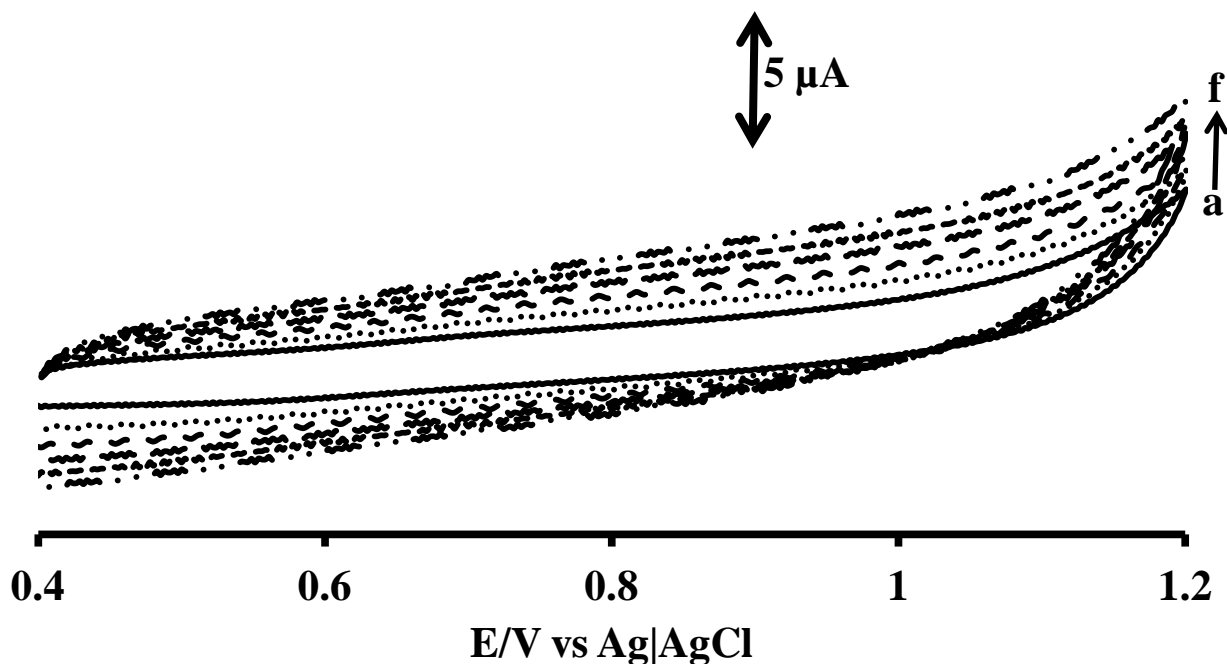
Figure 3.8: Cyclic voltammograms of CoTCPc/GONS-GCE in phosphate buffer pH 6 with increasing scan rate (a) 50 mV/s, (b) 100 mV/s, (c) 150 mV/s , (d) 200 mV/s, (e) 250 mV/s and (f) 300 mV/s.

Peak currents were sampled at 0.86 V to plot current against scan rate in Figure 3.9
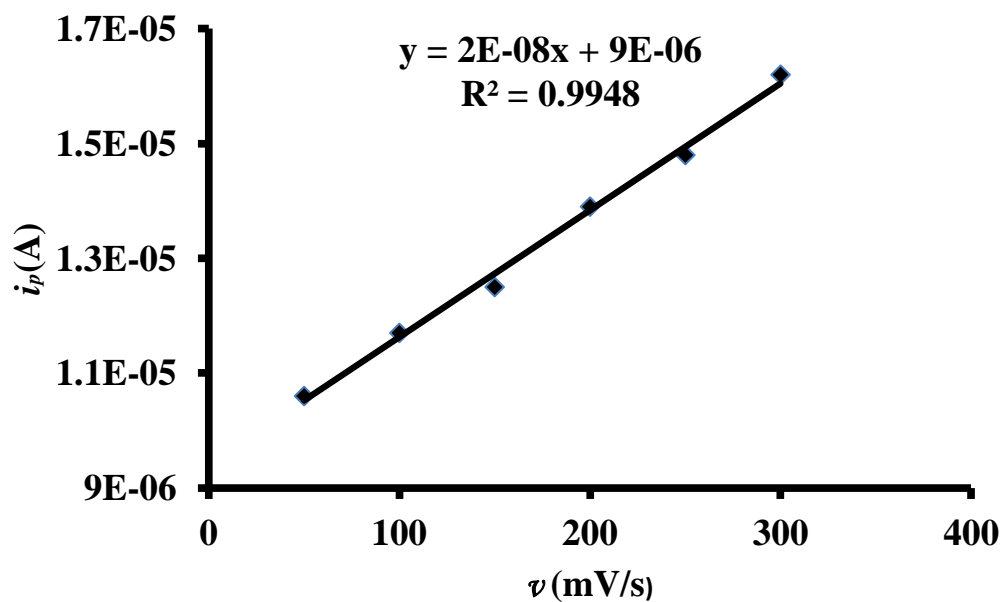
Figure 3.9: Plot of current against scan rate

From Equation (3.4) the plot of current against scan rate gives the Equation (3.5)

$$slope = (\frac{n^2 F^2 A}{4RT})\Gamma \qquad (3.5)$$

A surface coverage of 1.22×10^{-13} mol cm^{-2} was obtained.

3.2.6 Comparative study in 1 mM sodium nitrite in pH buffer 6
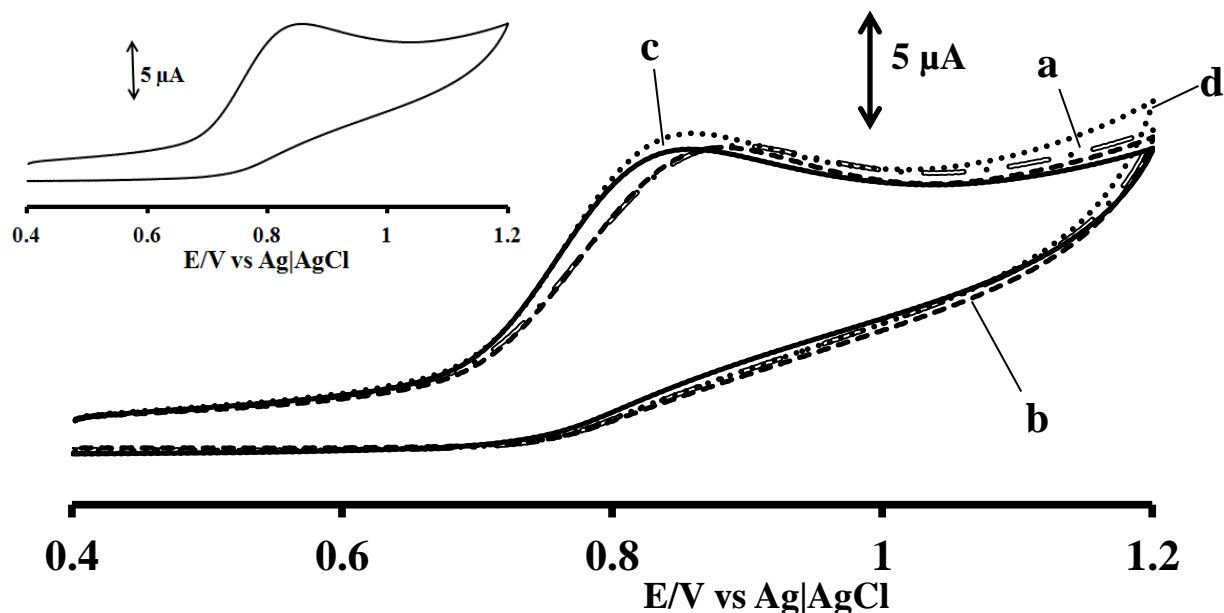
Figure 3.10: Cyclic voltammograms of:(a) BGCE , (b) CoTCPc-GCE , (c) N-GONS-GCE and (d) CoTCPc/N-GONS-GCE in 1 mM sodium Nitrite in pH 6 buffer. Inset BGCE. Scan rate = 50 mV/s

Figure 3.10 shows that the oxidation sodium nitrite started at a lower potential for CoTCPc/N-GONS-GCE, therefore the combination of cobalt phthalocyanine and nitrogen doped graphene had improved electrocatalytic property compared to the BGCE and other modifications. Current increased in the order CoTCPc/N-GONS-GCE< N-GONS-GCE< CoTCPc-GCE< BGCE.

Table 3.2: Peak currents, initial oxidation potential and peak oxidation potential for all probes, in 1 mM sodium nitrite in pH 6 buffer.

Electrode	Initial Oxidation Potential, E/V	Peak oxidation Potential, E/V	Current (µA)
BGCE	0.72	0.88	32.8
CoTCPc-GCE	0.71	0.87	34.8
N-GONS-GCE	0.68	0.85	35.2
CoTCPc/ N-GONS-GCE	0.66	0.84	35.5

Previous studies for the electrochemical determination of nitrites have been done using modified silver doped zeolite-expanded graphite-epoxy electrode and the oxidation potential was 0.90 V [2,96] . Comparing previous studies results with CoTCPc/N-GONS-GCE, it shows that it is the best electrode for the determination of nitrites.

3.2.7 Electrochemical Impedance Spectroscopy
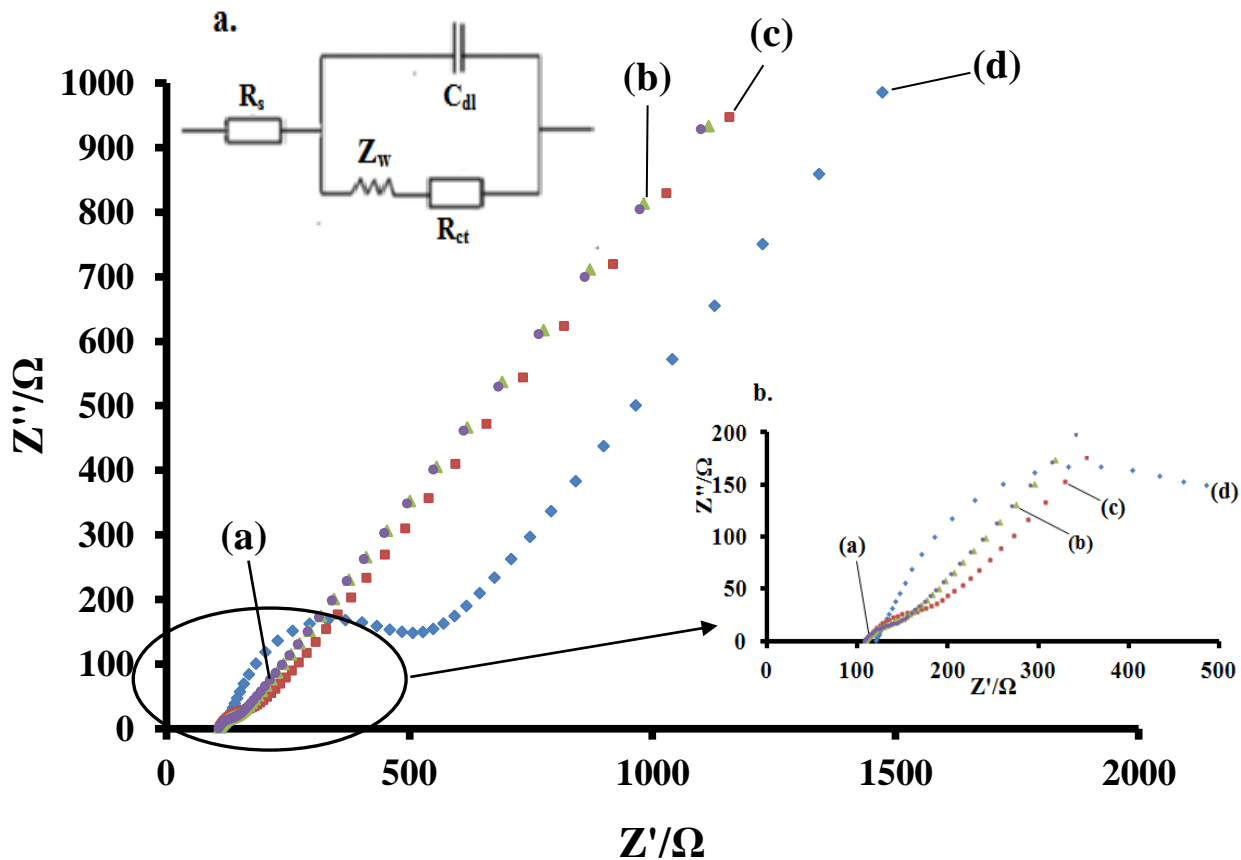
Figure 3.11: Nyquist plot of (a) CoTCPc/GONS-GCE, (b) N-GONS-GCE, (c) CoTCPc-GCE, (d) BGCE in 1 mM sodium nitrite (Phosphate buffer pH 6). Inset: (a) - Suggested Randles equivalent circuit model for the impedance spectrum (WE-working electrode, RE-reference electrode); (b) - Enlarged nyquist plot.

Further investigations were done using electrochemical impedance spectroscopy (EIS) in 1 mM sodium nitrite to deduce the electrochemical behaviour of the electrodes. The nyquist plots in Figure 3.11 of the four electrodes comprised of minute semicircles and straight line portions. The diameter of the semicircle corresponds to the charge transfer resistance and diffusion controlled

process respectively [97]. The straight line portion represents the Warburg impedance which takes into account the frequency dependence on diffusion transportation to the electrode surface [98]. The representative circuit for the Nyquist plots shown by inset in Figure 3.11(a) where, R_S, C_{dl}, R_{CT} and Z_W represent solution resistance, a constant phase element, the charge transfer resistance and the Warburg impedance respectively [99].

The apparent electron transfer rate constant (k_{app}) were obtained using Equation (3.6) [101];

$$k_{app} = \frac{RT}{F^2 R_{CT} C} \tag{3.6}$$

where C is the concentration of sodium nitrite (1 mM), with R, T and F having their usual meanings. As reflected in its k_{app} and R_{CT} values, CoTCPc/N-GONS-GCE exhibited fastest electron transfer process towards nitrite compared to other electrodes investigated in this research.

Table 3.3: Estimated parameters for the different electrodes.

Electrode	R_{CT} (Ω)	K_{app} (cms^{-1})
Bare GCE	484.74	5.49×10^{-7}
CoTCPc-GCE	181.33	1.47×10^{-6}
N-GONS-GCE	155.35	1.71×10^{-6}
CoTCPc/N-GONS-GCE	145.47	1.83×10^{-6}

The order of decrease of electron transfer efficiencies is as follows BGCE < CoTCPc-GCE< N-GONS-GCE < CoTCPc/N-GONS-GCE. The trend is the same as the one obtained in table 3.2 from the cyclic voltammetry study where CoTCPc/N-GONS-GCE exhibited reduced potentials and improved currents.

3.2.8 Kinetics
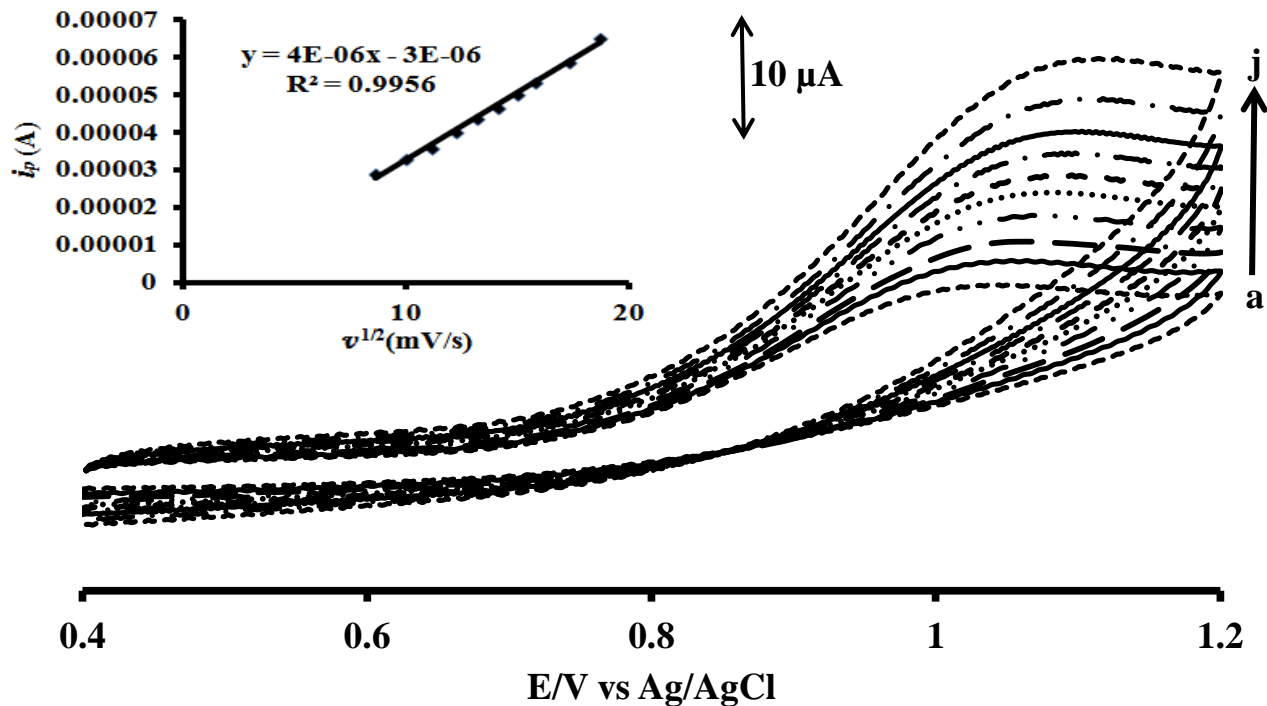
Figure 3.12: Cyclic voltammograms for CoTCPc/N-GONS-GCE in 1.0 mM sodium nitrite in pH 6 buffer. Scan rates: (a) 75 mV/s, (b) 100 mV/s, (c) 125 mV/s, (d) 150 mV/s, (e) 175 mV/s, (f) 200 mV/s, (g) 225 mV/s, (h) 250 mV/s, (i) 300 mV/s and (j) 350 mV/s. . Insert: Plot of peak current against square root of scan rate.

The effect of varying scan rate showed that the electro-catalytic oxidation of sodium nitrite was diffusion controlled [58,94,100], as shown by the insert, where the plot of peak current against scan rate showed linear relationship with a correlation value of 0.9956.
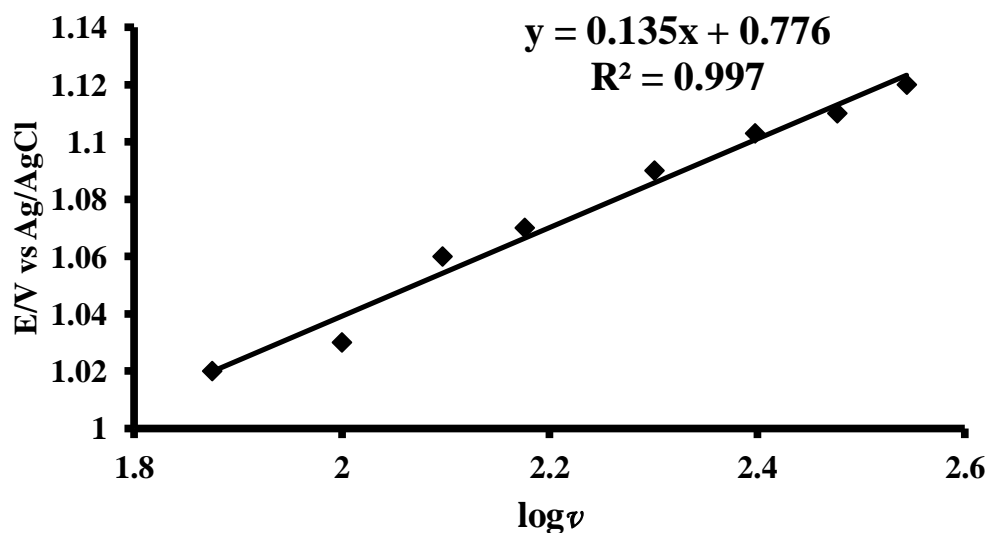
Figure 3.13: Plot of E_p against $\log v$

From the plot in Figure 3.13, a Tafel slope of 270 mV/ decade ($2 \times slope$) was produced. Such Tafel slopes have no kinetic meaning and are consistent with substrate-catalyst interaction in a reaction intermediate or simply passivation of the electrode surface [101]. Very high Tafel slopes, much greater than the normal of 30-120 mV/ decade for a one electron rate determining step are known and have been linked to chemical reactions coupled to electrochemical steps[25,98].

3.2.9 Order of reaction

Fig 3.14 is a plot of log l versus log [concentration] for sodium nitrite.
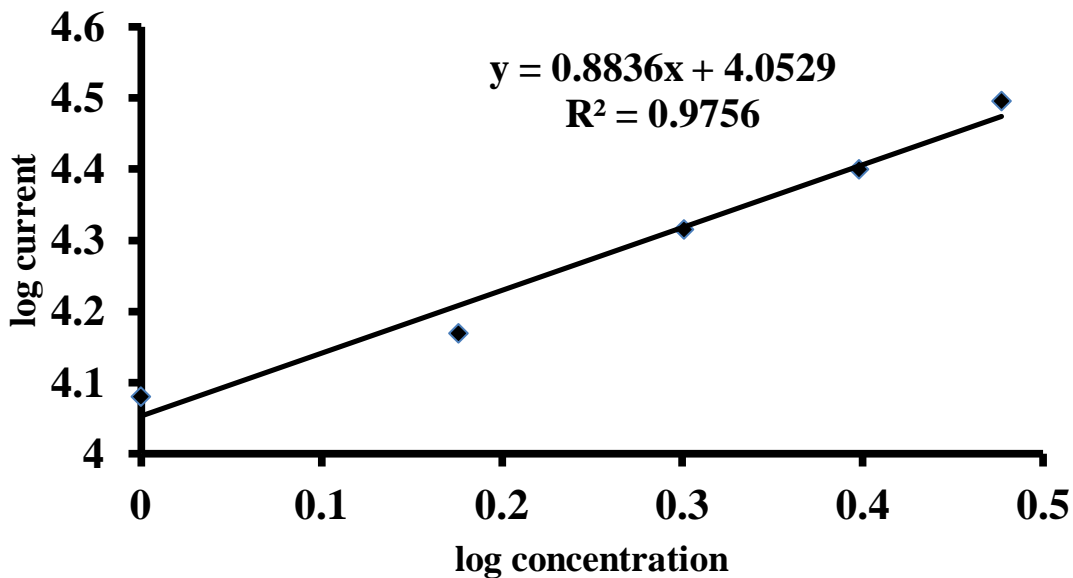
Figure 3.14: Plot of log current vs. log concentration of sodium nitrite

The slope from plot of log current vs log concentration gives the order of the reaction of the analyte [2]. From Figure 3.14 the slope is 0.8836 for the electro analysis of sodium nitrite, which is approximately equal to one, thus the catalytic oxidation of sodium nitrite is a 1st order reaction.

The proposed mechanism for the catalytic oxidation of sodium nitrite is given by Equation (3.7), (3.8) and (3.9);

$$Co^{III}Pc^{2-} \rightarrow Co^{III}Pc^{-} + e^{-} \tag{3.7}$$

$$Co^{III}Pc^{-} + NO_2^{-} \rightarrow Co^{III}Pc^{2-} + NO_2 \tag{3.8}$$

$$2NO_2 + H_2O \leftrightarrow NO_2^{-} + NO_3^{-} + 2H^{+} \tag{3.9}$$

3.2.10 Limit of detection

Differential pulse voltammetry was used to detect sodium nitrite at different concentrations, due to its ability to generate well defined peaks at low concentrations. The CoTCPc/N-GONS-GCE probe was used on different concentrations of sodium nitrite. The Relationship between the peak current and concentration is shown in Figure 3.15 insert.
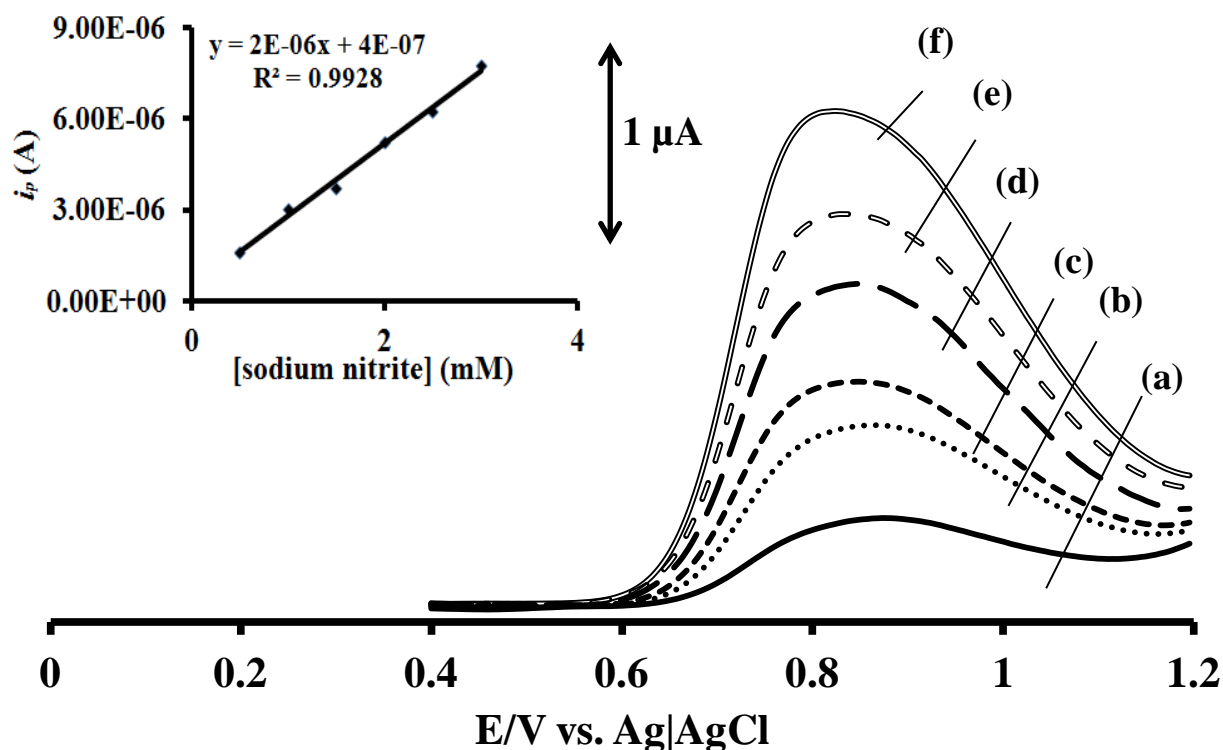
Figure 3.15: Differential pulse voltammetric determination of sodium nitrite at different concentrations: (a) 0.5 mM, (b) 1 mM, (c) 1.5 mM, (d) 2 mM, (e) 2.5 mM and (f) 3 mM. Insert: Plot of peak current against concentration. Scan rate = 100 mV/s.

The plot of peak current against concentration produced a linear relationship as shown in Figure 3.15 insert. The relationship was statistically analysed by the least square regression method. Calculations were done using the excel Linest formula. The linear regression equation was

obtained as $i_p = 2 \times 10^{-6} x + 4 \times 10^{-7}$ and $R^2 = 0.9928$, where x is he concentration of the analyte. The limit of detection is equivalent to $3\sigma/s$, where σ is the standard deviation of the intercept and s is the slope of the calibration curve. The limit of detection (LOD) was found to be 2.49×10^{-7} M, which lower than other reported researches for nitrite detection [2,22,23]. . The limit of quantification ($10\sigma/s$), for sodium nitrite was 8.29×10^{-7} M.

3.2.11 Reproducibility
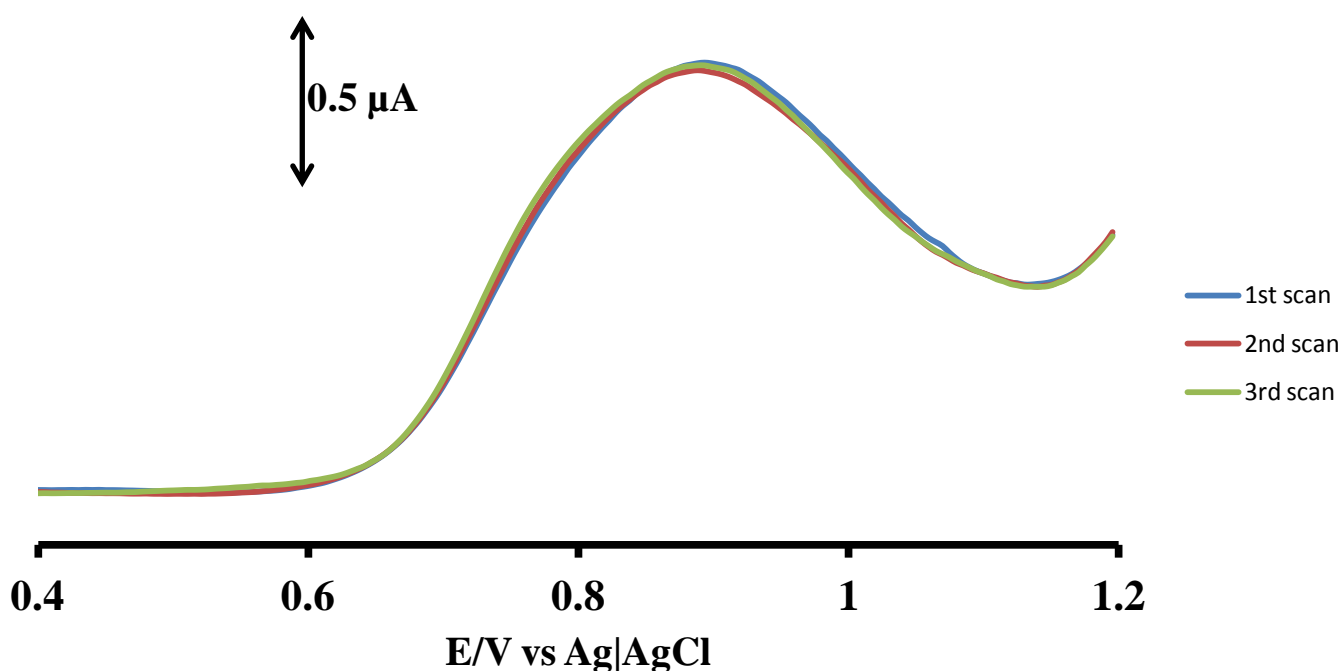
Figure 3.16: Differential pulse voltammograms for CoTCPc/N-GONS-GCE in 1 mM sodium nitrite in PBS (pH 6). Scan rate = 100 mVs^{-1}.

The CoTCPc/N-GONS-GCE was used to detect nitrites in 1 mM sodium nitrite for three times, in the same analyte concentration. The fabricated sensor was rinsed with distilled water before each run in order to remove any substrate on the electrode surface. There were slight

unnoticeable variations in the peak current upon each assay, with standard deviation of less than

zero. This indicated good reproducibility of the modified electrode [28,71].

3.2.12 Electrode stability
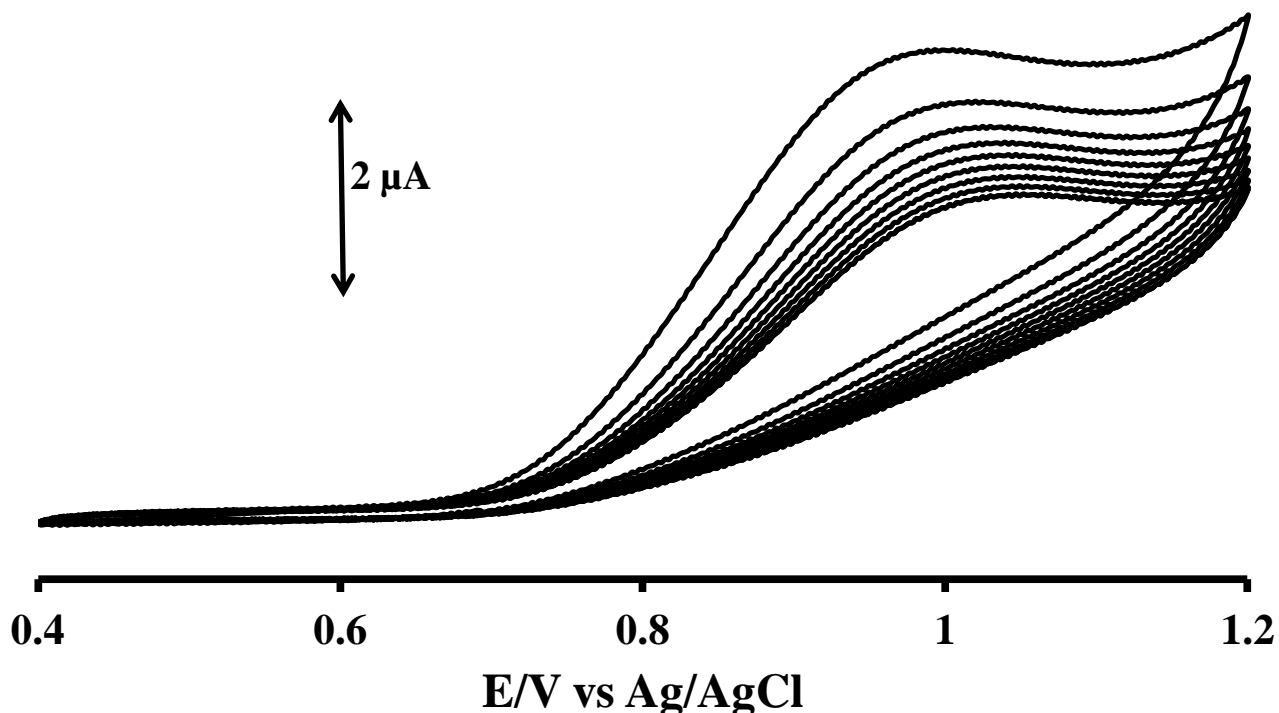
Figure 3.17: 20 continuous cyclic voltammetric evolutions in 1 mM sodium nitrite produced on CoTCPc/N-GONS-GCE. Scan rate = 100 mV/s. pH 6 buffer

From Figure 3.17 it is noted that peak current decreases as the number cycles continues, with the highest decrease between the first and the second scan and the drop in current becomes very small showing the passivation of the electrode. The rate at which current drops is a measure of resistance to passivation of the electrode towards the analyte [70]. There is an increase in the oxidation potential as the number of cycles continues and the highest differences are observed between the first and second scan. The increase becomes very small. The oxidation potential of

the first scan is lower than the second scan but it later becomes almost constant as the number of scans continues showing passivation of the electrode.

3.2.13 Interference studies
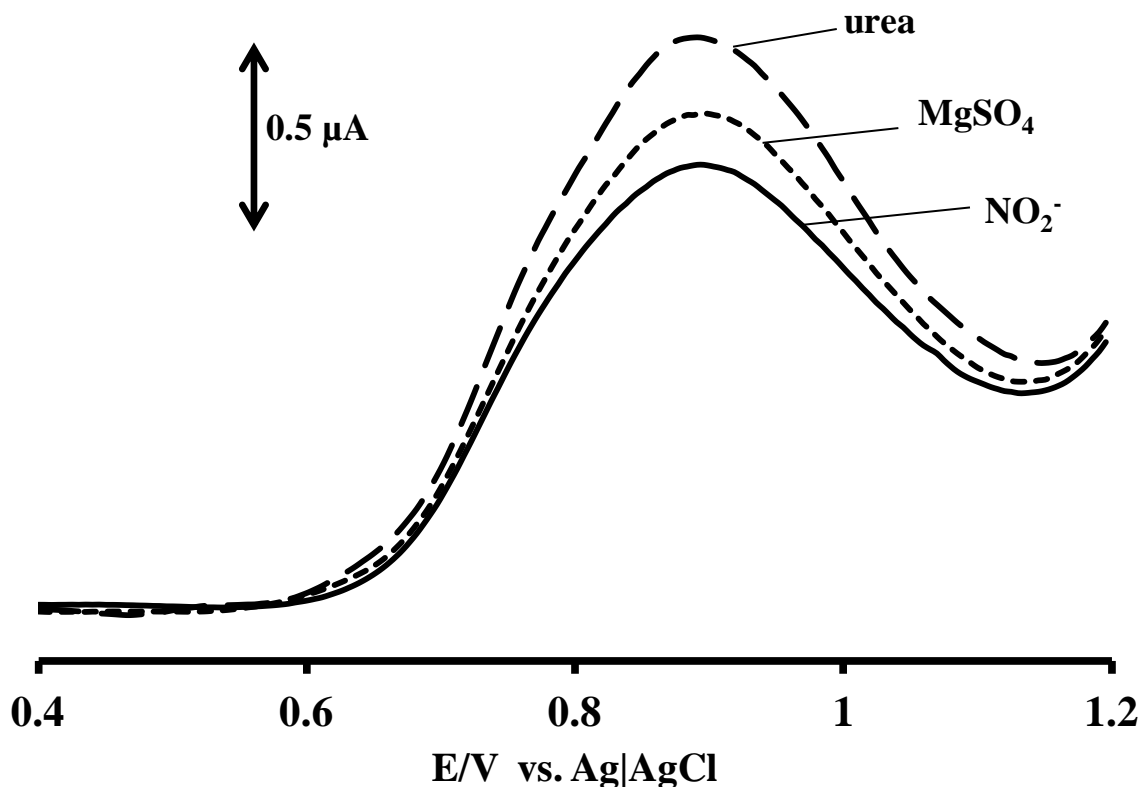
Figure 3.18: Differential pulse voltammograms of nitrite oxidation with and without interference. Scan rate 100 mV/s.

The selectivity of the CoTCPc/N-GONS-GCE towards 1 mM sodium nitrite was examined in the presence of other foreign species in 0.1 M PBS (pH 6). The species included magnesium sulphate and urea which were evaluated using DPV. The concentrations of the interfering compounds were in a 100 fold concentration [30]. The relative standard deviation (%) was calculated using the formulae;

$$RSD\ (\%) = 1 - (\frac{I_{pa}^{(analyte+inter)}}{I_{pa}^{analyte}}) \times 100 \tag{3.10}$$

where $I_{pa}^{analyte}$ and I_{pa}^{inter} are the peak currents for sodium nitrite and for the interfering respectively. Relative standard deviation (%) above 10% show that the compound interferes with the analyte. The RSD % were 23% for Urea and 8,7% for magnesium sulphate. The selected compounds showed that urea interferes with oxidation of sodium nitrite since the value was above 10%.

CHAPTER 4

4.0 Conclusion

CoTCPc nanopaticles were synthesised. The IR spectra and UV-Vis for results CoTCPc and N-GONS corresponded to similar compounds in literature. Further characterisation to evaluate the use of CoTCPc and N-GONS in the modification of glassy carbon electrode for the detection of nitrites was done and the results were successful in CV, DPV and EIS. The results showed that using CoTCPc and N-GONS can lower glassy carbon electrode oxidation potential of sodium nitrite.

The surface area of CoTCPc/N-GONS-GCE was 0.174 cm^2, which was twice that of a BGCE indicating that the modified electrode displayed an improved larger surface area for electrocatalysis. The surface coverage was 1.22×10^{-13} mol cm^{-2}, showing the deposited modifier on the electrode surface. The CoTCPc/N-GONS-GCE exhibited fastest electron transfer process towards nitrites compared to other electrodes investigated in this work as reflected in its k_{app} and R_{CT} values of 1.83×10^{-6} cms^{-1} and 145.47 Ω. The electrochemical detection of nitrites with CoTCPc/N-GONS-GCE was successful producing high peak currents compared to other electrodes. The catalytic oxidation of nitrites was found to be a 1st order reaction with a Tafel slope of 270 mV/ decade. Peak current increased with increasing nitrite concentration, while peak potential reduced. LOD was 2.49×10^{-7} M and LOQ was 8.29×10^{-7} M. The electrode showed good stability, sensitivity and reproducibility with lower oxidation potential at 0.86 V.

4.1 Recommendations

Further studies can be carried out by introducing large functional groups onto the CoPc ring, groups such as alkyl or aryl groups can be used so as to observe their effect on the electrocatalytic activities of the nitrites. Effect of temperature and accumulation time can also be studied. I recommend the use of CoTCPc/N-GONS-GCE for the detection of nitrites in the water works industry and mineral water bottlers.

REFERENCES.

[1]   Salimi A, Noorbakhash A, Karonian FS. Amperometric detection of Nitrite , Iodate and Periodate on Glassy Carbon Electrode modified with Thionin and Multi-wall Carbon Nanotubes 2006;1:435–45.

[2]   Afkhami A, Madrakian T, Ghaedi H, Khanmohammadi H. Electrochimica Acta Construction of a chemically modified electrode for the selective determination of nitrite and nitrate ions based on a new nanocomposite. Electrochim Acta 2012;66:255–64.

[3]   Gill AF. Insights into Sulfonated Phthalocyanines ; Insights into Anionic Tetraaryl Porphyrins ; Irradiation of Cationic Metalloporphyrins Bound to DNA 2006;34:364-69.

[4]   Phthalocyanines I, Uv SU, Mpf- PEF. 50 Years of Chemistry in Opole Octacarboxyphthalocyanines – compounds of interesting spectral , photochemical and catalytic properties 50 Years of Chemistry in Opole 2014;37:4–7.

[5]   Pillay J, Vilakazi S. Nanostructured metallophthalocyanine complexes : synthesis and electrocatalysis 2012;01:785–92.

[6]   Zhang Y, Fan Y, Cheng L, Fan L, Wang Z, Zhong J, et al. Electrochimica Acta A novel glucose biosensor based on the immobilization of glucose oxidase on layer-by-layer assembly film of copper phthalocyanine functionalized graphene 2013;104:178–84.

[7]   Guidelines WHO, Quality D. Nitrate and nitrite in drinking-water. 2009;11:22-7

[8]   Keeley GP, Neill AO, Mcevoy N, Peltekis N, Coleman N, Duesberg GS. Electrochemical ascorbic acid sensor based on DMF-exfoliated graphene.2015;07:77

[9]   Lee T, Jeon EK, Kim B. Mussel-Inspired Nitrogen Doped Graphene Nanosheets Supported Manganese Oxide Nanowires as Highly Efficient Electrocatalysts for Oxygen Reduction Reaction 2013;07:1–7.

[10] Mamuru SA, Ozoemena I. Heterogeneous Electron Transfer and Oxygen Reduction Reaction at Nanostructured Iron (II) Phthalocyanine and Its MWCNTs Nanocomposites 2010;09:985–94.

[11] Wei Q, Tong X, Zhang G, Qiao J, Gong Q, Sun S. Nitrogen-Doped Carbon Nanotube and Graphene Materials for Oxygen Reduction Reactions 2015;15:1574–602. .

[12] Shao Y, Zhang S, Engelhard MH, Li G, Shao G, Wang Y, et al. Nitrogen-doped graphene and its electrochemical applications 2010;20:7491–6.

[13] Deepan PG, Nisha NG, Karthigeyan A. Synthesis and characterization of nitrogen-doped graphene sheets by hydrothermal reduction method 2015;7:1553–8.

[14] Sharifi T. Efficient Electrocatalysts Based on Nitrogen-doped Carbon Nanostructures for Energy Applications. 2015;13:546-9.

[15] Xue Y, Chen H, Qu J, Dai L. Nitrogen-doped graphene by ball-milling graphite with melamine for energy conversion and storage. 2002;11:441-4.

[16] Mani V, Devasenathipathy R, Chen S, Gu J. Synthesis and characterization of graphene-cobalt phthalocyanines and graphene-iron phthalocyanine composites and their enzymatic fuel cell application. Renew Energy 2015;74:867–74.

[17] Canty R, Gonzalez E, Macdonald C, Osswald S, Zea H, Luhrs CC. Reduction Expansion Synthesis as Strategy to Control Nitrogen Doping Level and Surface Area in Graphene 2015;66:7048–58.

[18] Chang K, Geng D, Li X, Yang J, Tang Y, Cai M, et al. Ultrathin MoS 2 / Nitrogen-Doped Graphene Nanosheets with Highly Reversible Lithium Storage 2013;11:1–6.

[19] Wang G, Jia L, Zhu Y, Hou B, Li D, Sun Y. Novel preparation of nitrogen-doped graphene in various forms with aqueous ammonia under mild conditions 2012;20:20-38.

[20]   Albanese D, Di M, Alessio C. Screen printed biosensors for detection of nitrates in drinking water 2010;23;123-5.

[21]   Enzymol M, Enzymol M, Enzymol M, Enzymol M Electrochemical Detection of Nitric Oxide in Biological Fluids 2005;396:68–77.

[22]   Acta M. Electrochemical sensing of nitrite using a glassy carbon electrode modified with reduced functionalized graphene oxide decorated with flower-like zinc oxide . Microchim Acta Electrochemical sensing of nitrite using a glassy carbon electrode modified with 2016;03:34-8.

[23]   Adekunle AS, Mamba BB, Agboola BO, Ozoemena KI, Africa S. Nitrite Electrochemical Sensor Based on Prussian Blue / Single- Walled Carbon Nanotubes Modified Pyrolytic Graphite 2011;6:4388–403.

[24]   Mugadza T, Nyokong T. Electrochemical , microscopic and spectroscopic characterization of benzene diamine functionalized single walled carbon nanotube-cobalt (II) tetracarboxy-phthalocyanine conjugates 2011;354:437-47 .

[25]   Maringa A, Mugadza T, Antunes E, Nyokong T. Characterization and electrocatalytic behaviour of glassy carbon electrode modified with nickel nanoparticles towards amitrole detection. J Electroanal Chem 2013;700:86–92.

[26]   Bard AJ. Chemical Modification of Electrodes 1983;13:302–4.

[27]   Moyo M, Okonkwo JO. Sensors and Actuators B : Chemical Horseradish peroxidase biosensor based on maize tassel – MWCNTs composite for cadmium detection 2014;193:515-521.

[28]   Xian H, Wang P, Zhou Y, Lu Q. Electrochemical determination of nitrite via covalent immobilization of a single-walled carbon nanotubes and single stranded deoxyribonucleic

acid nanocomposite on a glassy carbon electrode 2010;171:63–9.

[29] Nanostructures and Metallophthalocyanines : Applications in Microbial Fuel Cells A thesis submitted in fulfillment of the requirements for the degree of MASTERS IN SCIENCE of by SEAN EDWARDS December 2010 .

[30] Ning D, Zhang H, Zheng J. Electrochemical sensor for sensitive determination of nitrite based on the PAMAM dendrimer-stabilized silver nanoparticles. J Electroanal Chem 2014;717-718:29–33.

[31] Sivaprasad M, Nagaraju M, Sreedhar NY, Pradesh A. Glassy carbon electrode modified with cobalt phthalocyanine and graphene composites for electroanalysis of bromfenvinfos and 2013;3:11–22.

[32] Yilong Z, Dean Z, Daoliang L. Electrochemical and Other Methods for Detection and Determination of Dissolved Nitrite. 2015;10:1144–68.

[33] Raoof JB, Ojani R, Beitollah H. Electrocatalytic determination of ascorbic acid at chemically modified Carbon paste electrode with 2, 7-bis (Ferrocenyl ethynyl) fluoren-9-one. Int J Electrochem Sci 2007;2:534–48.

[34] Talanta The effects of carbon nanotubes on the electrocatalysis of hydrogen peroxide by metallo-phthalocyanine. 2011;85:2202-11.

[35] Mugadza T, Nyokong T. Journal of Colloid and Interface Science Electrochemical , microscopic and spectroscopic characterization of benzene diamine functionalized single walled carbon nanotube-cobalt (II) tetracarboxy-phthalocyanine conjugates. J Colloid Interface Sci 2011;354:437–47.

[36] Mugadza T, Nyokong T. Electrochimica Acta Synthesis and characterization of electrocatalytic conjugates of tetraamino cobalt (II) phthalocyanine and single wall

carbon nanotubes 2009;54:6347–53.

[37] SYNTHESIS OF ZINC PHTHALOCYANINE DERIVATIVES FOR POSSIBLE USE IN PHOTODYNAMIC THERAPY THESIS 2002.

[38] Jain NC. The Pilgrimage of the Wonder Macromolecule : Phthalocyanine 2011;1:1–5.

[39] Fatemeh Ghani. Nucleation and Growth of Unsubstituted Metal Phthalocyanine Films from Solution on Planar Substrates 2012;01:35.

[40] Sook BR. I . Characterization of Sulfonated Phthalocyanines by Mass Spectrometry . II . Characterization of SlAA , a Streptococcal Heme-Binding Protein Associated with a Heme ABC Transport System 2008;01:64 -71.

[41] Sakamoto K, Ohno-okumura E. Syntheses and Functional Properties of Phthalocyanines 2009;02:1127–79.

[42] Engel MK, Complexes P, Engel MK. Single-Crystal and Solid-State Molecular Structures of Phthalocyanine Complexes . Michael K . Engel , Kawamura Rikagaku Kenkyusho Hokoku Single-Crystal and Solid-State Molecular Structures of 1997;13:11–54.

[43] Cui L, Chen L, Xu M, Su H, Ai S. Analytica Chimica Acta Nonenzymatic amperometric organic peroxide sensor based on nano-cobalt phthalocyanine loaded functionalized graphene film. Anal Chim Acta 2012;712:64 –71.

[44] Walter MG, Rudine AB, Wamser CC. Porphyrins and phthalocyanines in solar photovoltaic cells 2010;14:759 –92.

[45] McGrath D.Technology UAID. Peripheral and Non-Peripheral Substituted Phthalocyanines. 2011;1:110 - 118

[46] Warren A. Introduction to spectrometry 1999;11:1–10.

[47] Nyoni S, Mugadza T, Nyokong T. Improved l-cysteine electrocatalysis through a

sequential drop dry technique using multi-walled carbon nanotubes and cobalt tetraaminophthalocyanine conjugates. Electrochim Acta 2013;128:32-40

[48] Ncb EM. Copper phthalocyanine 1993;147:14-8 .

[49] Naturwissenschaften D. Binuclear Phthalocyanines : Synthesis , Characterisation and Optical Limiting Properties Binukleare Phthalocyanine : Synthese , 2004;01:10 - 15.

[50] Ascanio AMD, et al. A study of solvent and metal effects on formation of phthalocyanine at room temperature.1999;01:31- 9.

[51] Hipps KW, Mazur U. Electron affinity states of metal supported phthalocyanines measured by tunneling spectroscopy 2012:16:1– 9.

[52] Schuddeboom LS. Nitrates and nitrites in food stuff. 1993;01:4-7

[53] Electrocatalytic Detection of Pesticides with Electrodes Modified with Nanoparticles of Phthalocyanines and Multiwalled Carbon Nanotubes DOCTOR OF PHILOSOPHY (SCIENCE) OF By Msimelelo Patrick Siswana February 2010

[54] Kockrick E, Lescouet T, Kudrik E V, Sorokin AB. Synergetic effects of encapsulated phthalocyanine complexes in MIL-101 for the selective aerobic oxidation of tetralin 2011;16:66 - 8.

[55] Ward J.R, Seider RP, Aggregation of cobalt (II) tetra sulfonated phthalocyanine in methanol water solution. 1983;8:16-27

[56] Mashazi PN, Westbroek P, Ozoemena KI, Nyokong T. Surface chemistry and electrocatalytic behaviour of tetra-carboxy substituted iron , cobalt and manganese phthalocyanine monolayers on gold electrode 2007;53:1858–69.

[57] Jian cheng Z. Ultraviolet - Visible Spectroscopy (UV) , of cobalt phthalocyanine. 2014;03:1 - 7

[58] Ortiz B, Park S. Electrochemical and Spectroelectrochemical Studies of Cobalt Phthalocyanine Polymers 1996;143:1800–5.

[59] Higaki S, Hanabusa K, Shirai H, Hojo N. Functional Metal-porphyrazine Derivatives and Their tetracarboxyphthalocyanine Covalently Bound to Poly (2- or 4-vinylpyridine-co-styrene) 1983;699:691–9.

[60] Jian-ming C, Jian-cheng Z, Yue S, Xiu-hong LIU, Lin-hong Y. Preparation and Photoconductivity of Fe-Phthalocyanine Derivation and C6o Composite Films 2000;5:432-7.

[61] Wiley J. Analytical Electrochemistry ,2nd edition . New York. 2009:1996–7.

[62] Tio M. Electrochemical methods. 1942;11:280 - 9

[63] Petrauskas K, Baronas R. Computational Modeling of Mediator Oxidation by Oxygen in an Amperometric Glucose Biosensor 2014; 21:2578 –94.

[64] Harvey D. Modern analytical chemistry, 2nd edition, New York. 2011; 129-39

[65] Monk P, Wiley J. Fundamental electro- analytical chemistry, 4th edition. Manchester, UK, 85 -103.

[66] Kasem BKK, Jones S. Platinum as a Reference Electrode in Electrochemical Measurements 2008;2:100–6.

[67] Theoretical Background of Electrochemical Analysis 2013;04:978 - 983.

[68] Choi H, Yoon H. Nanostructured Electrode Materials for Electrochemical Capacitor Applications 2015;05:906–36.

[69] Yan Z, Li H. Voltammetric Determination of 6-mercaptopurine at Co (III) Trisphenanthroline Complex and DNA Decorated with Grpahene Oxide Modified Glassy Carbon Electrode 2015;10:8714–26.

[70] Fischer J, Vanourkova L, Danhel A, Vyskocil V, Cizek K, Barek J, et al. Voltammetric Determination of Nitrophenols at a Silver Solid 2007;2:226–34.

[71] Ramachandran R, Mani V, Chen S, Gnana G. Recent Developments in Electrode materials and Methods for Pesticide Analysis - An overview 2015;10:859–69.

[72] Ndlovu T, Arotiba OA, Sampath S, Krause RW, Mamba BB. Reactivities of Modified and Unmodified Exfoliated Graphite Electrodes in Selected Redox Systems 2012;7:9441–53.

[73] March G, Dung T, Piro B. Modified Electrodes Used for Electrochemical Detection of Metal Ions in Environmental Analysis 2015;06:241–75.

[74] Segura RA, Pizarro JA, Oyarzun MP, Castillo AD, Díaz KJ, Placencio AB. Determination of Lead and Cadmium in Water Samples by Adsorptive Stripping Voltammetry Using a Bismuth film / 1- Nitroso-2-Napthol / Nafion Modified Glassy Carbon Electrode 2016;11:1707–19.

[75] Kuprum P, Menggunakan II, Perlucutan V, Denyut A. Differential pulse anodic stripping voltammetry determination of copper (ii) at glassy carbon electrode in the presence of bis (benzylidene) ethylenediamine as a novel complexing agent 2015;19:309–17.

[76] Baciu A, Ardelean M, Pop A, Pode R, Manea F. Simultaneous Voltammetric/Amperometric Determination of Sulfide and Nitrite in Water at BDD Electrode 2015;13:14526–38.

[77] García-cruz L, Sáez A, Ania CO, Solla-gullón J. Electrocatalytic activity of Ni-doped nanoporous carbons in the electrooxidation of propargyl alcohol. 2010;147:645 -52.

[78] Adekunle AS, Pillay J, Ozoemena KI. physiological pH conditions. Electrochim Acta 2009;16:102 - 107.

[79] Geraldo DA, Limson J, Nyokong T. Electrochimica Acta Electrooxidation of hydrazine

catalyzed by noncovalently functionalized single-walled carbon nanotubes with CoPc 2008;53:8051–7.

[80] Lomova TN, Klyueva ME, Yu E, Bichan NG. Use of chemical kinetics for the description of metal porphyrin reactivity 2012;16:1040–54.

[81] Ii F. Functional Metal-porphyrazine Derivatives and Their Polymers, 1980;1012:1003–12.

[82] Wang C. Detection of chemical pollutants in water using gold nanoparticles as sensors 2012;32:1 -14.

[83] Suni II. Impedance methods for electrochemical sensors using nanomaterials 2008;27: 604 - 605.

[84] Bernal J, Politécnica U, Mexiquense A, Villa C, P TEDMC, Juanico A, et al. Current Status of Nanotechnology in México Nanonechnology Industries and Commerce in Mexico.2000;07:54–60.

[85] Neha B, Manjula KS, Srinivasulu B, Subhas SC. Synthesis and Characterization of Exfoliated Graphite / ABS Composites 2012;12:74–8.

[86] Duan PDX, Poeppelmeier LHGKR, Sauvage GPJ. Structure and Bonding Series Editor : D . M . P . Mingos Editorial Board : n.d.

[87] Wang C. Dithiooxamide Modified Glassy Carbon Electrode for the Studies of Non-Aqueous Media: Electrochemical Behaviors of Quercetin on the Electrode Surface 2012;42:3916–28.

[88] Yu E, Bichan NG Electrochemical determination of nitrites. 2002;23:211 -15 .

[89] Mandil A, Pauliukaite R, Amine A, Brett CMA. Electrochemical characterization of and stripping voltammetry at screen printed electrodes modified with different brands of multiwall carbon nanotubes and bismuth films 2012;10:395–407.

[90] Stuat S, Wiley J. Infrared spectroscopy fundamental and application. 2004;07:10 - 23.

[91] Wang C. A highly nitrogen-doped porous graphene - an anode material for lithium ion batteries 2015;3:1229–37.

[92] Ogunlusi GO, Adekunle AS, Maxakato NW, Mamba BB. Characterization of a Nano-synthesised Cobalt Complex and its Electrocatalytic Properties towards Nitrite Oxidation 2012;7:2904–17.

[93] Unter KT, Luedtke NW, Alzeer J. Synthesis and Evaluation of Guanidino Phthalocyanines for G-quadruplex Binding 2008;06:19 - 26.

[94] Mugadza T, Nyokong T. Synthesis and electrocatalytic behavior of cobalt -tris(benzyl-mercapto)-monoaminophthalocyanine single walled carbon nanotube nanorods. Electrochim Acta 2010:442 - 449

[95] Salimi A, Hallaj R, Mamkhezi H, Soltanian S . Electrochemical properties and electrocatalytic activity of FAD immobilised onto cobalt oxide nanoparticles: Application to nitrite detection. 2009;619 -620:31 - 38.

[96] Manea F, Remes A, Radovan C, Pode R, Picken S, Schoonman J. Talanta Simultaneous electrochemical determination of nitrate and nitrite in aqueous solution using Ag-doped zeolite-expanded graphite-epoxy electrode. 2010;83:66–71.

[97] Mugadza T, Arslano Y. Single walled carbon nanotube conjugate platforms and their use in electrocatalysis of amitrole. 2012;68:48 - 51

[98] Maringa A, Mugadza T, Antunes E, Nyokong T. Characterization and electrocatalytic behaviour of glassy carbon electrode modified with nickel nanoparticles towards amitrole detection 2013;100: 87 - 90.

[99] Mugadza T, Nyokong T. Synthesis and electrocatalytic behavior of cobalt (II)-tris(benzyl-

mercapto)-monoaminophthalocyanine-single walled carbon nanotube nanorods. Electrochim Acta 2011: 438 - 443.

[100] Mugadza T, Nyokong T. Electrochimica Acta Electrocatalytic oxidation of amitrole and diuron on iron (II) tetraaminophthalocyanine-single walled carbon nanotube dendrimer 2010;55:2606–13.

[101] Mugadza T, Nyokong T. Covalent linking of ethylene amine functionalized single-walled carbon nanotubes to cobalt (II) tetracarboxyl-phthalocyanines for use in electrocatalysis. 2010;160:2090 - 2093.

APPENDIX A: MATERIALS
List A1: Apparatus used for synthesis and characterisation

Beakers, volumetric flasks (100 ml, 250 ml, 500 ml, 1000 ml), burette, spatula, pestle and mortar, sample bottles (500 ml), filter funnels, conical flasks, weighing crucibles, measuring cylinder (10 ml, 50 ml, 100 ml),whattman filter papers, Erlenmeyer flask, Liebig's condenser, distillation flask.

Table A1: Reagents and chemicals.

Name	Chemical formula	Manufacturer	Concentration/Mass
Trimellitic acid anhydride	$C_9H_4O_5$	Sigma Aldrich	4.79 g
Cobalt (II) chloride	$CoCl_2.6H_2O$	Alpha Chemika	3.71 g
Ammonium chloride	NH_4Cl	Merck Chemicals	0.27 g
Ammonium molybdate	$(NH_4)_2MoO_4$	Glass world	0.59 g
Urea	$CO(NH_2)_2$	Radchem	15.0 g
Nitrobenzene	$C_6H_5NO_2$	Alpha Chemika	2 M
Ethanol	C_2H_5OH	Cosmo chemicals	99%
Hydrochloric acid	HCl	Skylabs	85 %
Sodium hydroxide	$NaOH$	Skylabs	0.1 M
Sodium chloride	$NaCl$	Merck Chemicals	0.1 M
Methanol	CH_3OH	ACE	95%
Sodium nitrite	$NaNO_2$	Minema	0.1 M

Phosphoric acid	H_3PO_4	Merck chemical	0.1 M
di Sodium hydrogen phosphate	Na_2HPO_4	Merck chemical	0.1 M
Dimethyl sulfoxide	C_2H_6OS	ACE	2 M
Potassium dihydrogen phosphate	KH_2PO_4	Merck chemical	0.1 M
Potassium bromide	KBr	Skylabs	0.01 g
Potassium chloride	KCl	Skylabs	1 M
Distilled water	H_2O	MSU labs	-

Table A 2: Instrumentation.

Name	Model	Manufacturer	Use in research
Analytical Balance	JJ 224 BC	G and G	Weighing
FTIR	Nicolet 6700	Thermoscientific	Characterisation
pH meter	Orion star- A 211	Labotec	pH measurement
Potentiostat	PGSTAT302N	AUTO LAB	Electroanalysis
UV-vis	UV-1700	Shimadzu	UV spectra
Sonicator	KQ-250B	China Corp.	Ultra-agitation

Treatment of Glassware

Laboratory detergents were used to wash glassware after which they were rinsed using distilled water to remove contaminants and impurities. This would help minimise interference that could occur during analyses.

APPENDIX B: UV-Vis spectra data.

Wavelength	CoTCPc Absorbance	N-GONS Absorbance	CoTCPc/N-GONS Absorbance
200	0.73	0.728	0.729
210	0.967	0.965	0.966
220	0.976	0.974	0.975
230	0.937	0.936	0.937
240	1.033	1.032	1.032
250	1.012	1.01	1.011
260	0.952	0.95	0.95
270	0.878	0.877	0.876
280	0.837	0.837	0.836
290	0.823	0.816	0.819
300	0.756	0.664	0.712
310	0.567	0.39	0.479
320	0.505	0.234	0.374
330	0.47	0.137	0.322
340	0.415	0.088	0.28
350	0.424	0.074	0.279
360	0.375	0.065	0.243
370	0.297	0.063	0.189
380	0.225	0.061	0.142

390	0.164	0.043	0.095
400	0.142	0.055	0.087
410	0.107	0.055	0.064
420	0.08	0.054	0.046
430	0.067	0.059	0.039
440	0.058	0.057	0.034
450	0.045	0.055	0.026
460	0.036	0.052	0.02
470	0.031	0.054	0.026
480	0.026	0.051	0.013
490	0.024	0.048	0.011
500	0.023	0.05	0.01
510	0.024	0.051	0.011
520	0.026	0.049	0.012
530	0.03	0.052	0.014
540	0.037	0.054	0.017
550	0.05	0.055	0.023
560	0.067	0.05	0.025
570	0.09	0.048	0.028
580	0.116	0.046	0.032
590	0.16	0.047	0.044
600	0.241	0.042	0.057

610	0.32	0.042	0.08
620	0.303	0.043	0.129
630	0.3	0.044	0.181
640	0.35	0.043	0.162
650	0.454	0.042	0.156
660	0.633	0.043	0.181
670	0.768	0.041	0.238
680	0.833	0.038	0.356
690	0.73	0.042	0.533
700	0.383	0.041	0.618
710	0.167	0.039	0.504
720	0.086	0.038	0.242
730	0.053	0.037	0.101
740	0.034	0.036	0.049
750	0.021	0.035	0.028
760	0.015	0.035	0.016
770	0.011	0.034	0.007
780	0.009	0.037	0.003

APPENDIX C: CALCULATIONS

C 1: Effective surface area (A_{eff})

Constant R = 8.314 Jmol-1, T = 273 K

Rearranging Randles-Sevcik equation

$$A_{eff} = m/((2.69 \times 10^5)n^{\frac{3}{2}}D^{\frac{1}{2}}C)$$

where D = 7.6×10^{-6} cm^2 s^{-1}, n = 1, m = 0.6441, C = 0.005 M and A$_{eff}$ = 0.174 cm^2.

C 2: Surface coverage/ Γ

$$slope = (\frac{n^2F^2A}{4RT})\Gamma$$

Constant R = 8.314 Jmol-1, T = 273 K

where A$_{eff}$ = 0.174 cm^2, n = 1, F = 96487 C/ mol and Γ =1.12 $\times10^{-5}$ mol/cm^2.

C 3: Limit of Detection (LOD) and Limit of Quantification (LOQ)

Table C1: Excel Linest function.

	Coefficients	Standard Error
Intercept	4.00667$\times 10^{-7}$	1.98561$\times 10^{-7}$
X Variable 1	2.39486$\times 10^{-6}$	1.01971$\times 10^{-7}$

C4: Apparent rate constant (k$_{app}$)

$$k_{app} = \frac{RT}{F^2R_{CT}C} \quad , \text{Constant R = 8.314 Jmol-1, T = 273 K}$$

where C = 0.001 M.